

**PURDUE UNIVERSITY
GRADUATE SCHOOL
Thesis/Dissertation Acceptance**

This is to certify that the thesis/dissertation prepared

By Satyajeet Suresh Shinde

Entitled

Structural Optimization Of Thin Walled Tubular Structure For Crashworthiness

For the degree of Master of Science in Mechanical Engineering

Is approved by the final examining committee:

Dr. Andres Tovar

Dr. Sohel Anwar

Dr. Tamer Wasfy

To the best of my knowledge and as understood by the student in the *Thesis/Dissertation Agreement, Publication Delay, and Certification/Disclaimer (Graduate School Form 32)*, this thesis/dissertation adheres to the provisions of Purdue University's "Policy on Integrity in Research" and the use of copyrighted material.

Approved by Major Professor(s): Dr. Andres Tovar

Approved by: Dr. Sohel Anwar

03/12/2014

Head of the Department Graduate Program

Date

STRUCTURAL OPTIMIZATION OF THIN WALLED TUBULAR STRUCTURE FOR
CRASHWORTHINESS

A Thesis

Submitted to the Faculty

of

Purdue University

by

Satyajeet Suresh Shinde

In Partial Fulfillment of the

Requirements for the Degree

of

Master of Science in Mechanical Engineering

August 2014

Purdue University

Indianapolis, Indiana

Dedicated to my family and friends.

ACKNOWLEDGEMENTS

I would like to express my deepest gratitude to my advisor, Dr. Andrés Tovar for his invaluable time, guidance, motivation to better my work and constant supervision for the entire course of the research work. Most of all, I would like to thank him for having given me the opportunity to work under him and showing faith in my abilities. In this journey I have had so many invaluable lessons from him which would help me in my future.

I would like to acknowledge the members of my committee, Dr. Sohel Anwar and Dr. Tamer Wasfy for their invaluable suggestions and support that helped in improving this dissertation immensely.

I gratefully acknowledge Honda R&D Americas for their generous grant which helped me to pursue my research. I would like to acknowledge Duane Detwiler and Emily Nutwell from Honda R&D for sharing their expertise and providing guidance throughout.

I would like to thank the entire team of Engineering Design Research Laboratory team: Kunal Khadhe, Kai Liu, Anahita Emami, Josh Israel, Weigang An and Ashish Khanna for their help and encouragement.

At last I would like to thank my parents for their unconditional support and encouragement. I am grateful to my sister for always cheering me up and she stood by me through this exciting and challenging journey.

TABLE OF CONTENTS

	Page
LIST OF TABLES	vii
LIST OF FIGURES	viii
LIST OF ABBREVIATIONS	xi
ABSTRACT	xiii
CHAPTER 1. INTRODUCTION	1
1.1 Automotive Safety	1
1.2 Crashworthiness	3
1.2.1 Controlled Energy Absorption for Crashworthiness Design	5
1.2.2 Automotive Crashworthiness Requirements for a Body in Prime (BIP) ..	6
1.2.3 Design for Crashworthiness	8
1.2.4 Tubular Structures for Crashworthiness	9
1.3 State of the Art	11
1.3.1 Structural Optimization.....	11
1.3.2 Crashworthy Thin-Walled Tubular Structures.....	15
1.3.2.1 Crush Initiators.....	16
1.3.2.2 Tapered and Internal Cellular Structures	18
1.3.2.3 Foam Filled Structures	18
1.3.2.4 Design Methodology for Crashworthy Tubular Components.....	19
1.3.2.5 What is Missing?.....	20
1.4 Research Objective.....	20
1.4.1 Numerical Implementation of a Structural Synthesis Method for Crashworthiness	21
1.4.2 Structural Synthesis of Thin-Walled Tubular Components	21
1.4.3 Proposed Weighted Approach for Thin-Walled Tubular Component Synthesis	22
1.4.4 Original Contributions	23
CHAPTER 2. NUMERICAL IMPLEMENTATION OF STRUCTURAL SYNTHESIS FOR CRASHWORTHINESS USING HCA.....	24
2.1 Structural Optimization.....	24
2.2 Hybrid Cellular Automaton (HCA) Synthesis	26
2.2.1 Cellular Automata	27
2.2.2 Design Rules	30
2.2.3 HCA Algorithm.....	33
2.3 Numerical Results	34

	Page
2.3.1 Example 1: Topology Synthesis of a Bumper-Like Structure	34
2.3.2 Example 2: Topography Optimization of a Base Plate	36
2.3.3 Example 3: Force Invertor Design	37
CHAPTER 3. STRUCTURAL SYNTHESIS OF THIN-WALLED TUBULAR COMPONENTS.....	40
3.1 Technical Background	40
3.2 Proposed Design Methodology	43
3.3 Design Control Algorithm.....	50
3.4 LS-Dyna Model.....	51
3.5 Numerical Results	53
3.5.1 Proposed Benchmark Structures	52
3.5.2 Geometry Definition of a Complex Tubular Structure	59
3.6 Results	60
3.6.1 Tubular Structure with Geometric Imperfection.....	60
3.6.2 S-Rail with Geometric Imperfection.....	64
3.7 Summary of Contributions.....	67
CHAPTER 4. PROPOSED WEIGHTED APPROACH FOR THIN-WALLED TUBULAR COMPONENT SYNTHESIS	69
4.1 Technical Background	69
4.2 Proposed Design Methodology: Weighted Multi-Objective Approach.....	71
4.3 Numerical Results	74
4.4 Summary of Contributions.....	80
CHAPTER 5. SUMMARY AND RECOMMENDATIONS.....	81
5.1 Summary	81
5.1.1 Numerical Implementation of Structural Synthesis for Crashworthiness Using HCA	81
5.1.2 Structural Synthesis of Thin-Walled Tubular Components	82
5.1.3 Proposed Weighted Approach for Thin-Walled Tubular Component Synthesis	82
5.2 Original Contributions	83
5.3 Future Recommendation	83
LIST OF REFERENCES	85

LIST OF TABLES

Table	Page
Table 3-1 Material properties of steel used for tube models	52
Table 3-2 Comparison between Uniform tube, Designs 1 and 2.....	62

LIST OF FIGURES

Figure	Page
Figure 1-1	Motor vehicle crash deaths per 100,000 people by type, 1975-2012..... 1
Figure 1-2	Influence of Vehicle Design Improvements: Driver deaths per hundred thousand registered vehicles, actual death rates vs. hypothetical death rates based on 1985 vehicle design.2
Figure 1-3	Body in white (BIW) structure of a Car6
Figure 1-4	BIW structure showing S-Rail8
Figure 1-5	Energy absorbers to the bumper.....9
Figure 1-6	Progressive Buckling..... 10
Figure 1-7	Euler-type buckling 11
Figure 1-8	Various crush initiators 17
Figure 2-1	Typical 2-D neighborhoods for CA's. N is the number of neighboring CA's: (a) N = 0, (b) N = 4, (c) N = 8, (d) N = 2428
Figure 2-2	The corresponding 3-D neighborhoods for CA's. N is the number of neighboring CA's: (a) N = 0, (b) N = 6, (c) N = 26, (d) N = 12428
Figure 2-3	Illustration of HCA method for thickness optimization for crashworthiness design.....34
Figure 2-4	Topology optimization of a pumper like structure.....35
Figure 2-5	Box constraints for the topography design.....35
Figure 2-6	Topography optimization of a base plate37
Figure 2-7	Force Inverter Design problem.....38
Figure 2-8	Force inverter optimization results.....39
Figure 3-1	Typical force-displacement behavior for an axially crushed thin-walled square tube.41
Figure 3-2	Bending mode of collapse for an S-rail.....42

Figure	Page
Figure 3-3	Structural optimization set-up in a compliant mechanism design problem using the “dummy load” method.45
Figure 3-4	Location of input and output ports for a squared tubular structures following the wavelength λ corresponding to the progressive buckling after an idea axial crushing condition.45
Figure 3-5	Two load cases used for the design methodology.....48
Figure 3-6	Design control algorithm.....50
Figure 3-7	Stress-strain curve for the material used for the analysis.....52
Figure 3-8	Crushing load angle θ between a rigid moving wall and the thin-walled tubular structure.54
Figure 3-9	Wall angle β of a tapered structure.....55
Figure 3-10	Thickness angle α of a tubular structure.....55
Figure 3-11	Results for critical load angle, $\theta_{cr} = 32^\circ$56
Figure 3-12	Results for critical wall angle $\beta = 5.0^\circ$ critical angle $\theta_{cr} = 64$57
Figure 3-13	Results for critical wall angle $\alpha = 1.0^\circ$ critical angle $\theta_{cr} = 51^\circ$58
Figure 3-14	The geometry of the tubular structure with imperfection.....59
Figure 3-15	The geometry of the tubular structure with imperfection.....60
Figure 3-16	Euler buckling seen in tubular structures with imperfection.....61
Figure 3-17	Thickness distribution for Design 1 (top) and Design 2 (bottom)62
Figure 3-18	Results for the compliant tubular structure with imperfection.....63
Figure 3-19	Thickness distribution for designed tube.....64
Figure 3-20	Comparison between designs for axial impact case.....66
Figure 3-21	Comparison between designs for oblique impact case.....67
Figure 4-1	Load case’s for tubular weighted multi-objective approach.72
Figure 4-2	Tube with weight $w = 0$75
Figure 4-3	Tube with weight $w = 1$75
Figure 4-4	Tube with geometric imperfection subjected to an impact at angle α76
Figure 4-5	Plot of the weight (w) vs Oblique impact angle α76
Figure 4-6	Comparison between uniform thickness tube and designed tube subjected to the axial impact.....77

Figure		Page
Figure 4-7	Comparison between uniform thickness tube and designed tube subjected to oblique impact.....	78
Figure 4-8	Comparison between compliant mechanism approach and weighted multi-objective approach.....	79
Figure 5-1	Recommendation to extend the weighted multi-objective approach.	84

LIST OF ABBREVIATIONS

HCA	hybrid cellular automaton
CA	cellular automaton
I/P	input port
O/P	output port
MPE	mutual potential energy
MPE_i	element mutual potential energy
\widetilde{MPE}_i	effective element mutual potential energy
SE	strain energy
GA	geometric advantage
MA	mechanical advantage
d_{in}	input port displacement
d_{out}	output port displacement
k_{in}	input port spring constant
k_{out}	output port spring constant
F_{in}	input port force
F_{out}	output port reaction force
F_{max}	peak force
F_{mean}	mean force
w	Weighting factor in multi-objective optimization
\mathbf{F}_d	dummy force vector
\mathbf{U}_1	displacement vector for to input load
w	tube width
t	tube wall thickness
\mathbf{t}	tube thickness wall distribution

t_i	thickness wall of a discrete tube element
t_{\min}	lower thickness bound
t_{\max}	upper thickness bound
σ_{d_i}	element stress vector corresponding to the dummy load
ϵ_{1_i}	element strain vector corresponding to the input load
M	Mass
M_{\max}	upper limit in mass
n	number of design variables or finite elements
N_i	Neighborhood
r	neighborhood range
θ	impact angle between the moving rigid wall and the tube
θ_{cr}	critical impact angle
α	thickness angle
α_{cr}	critical thickness angle
β	wall angle
β_{cr}	critical wall angle

ABSTRACT

Shinde, Satyajeet Suresh. M.S.M.E., Purdue University, August 2014. Structural Optimization of Thin Walled Tubular Structure for Crashworthiness. Major Professor: Andres Tovar.

Crashworthiness design is gaining more importance in the automotive industry due to high competition and tight safety norms. Further there is a need for light weight structures in the automotive design. Structural optimization in last two decades have been widely explored to improve existing designs or conceive new designs with better crashworthiness and reduced mass. Although many gradient based and heuristic methods for topology and topometry based crashworthiness design are available these days, most of them result in stiff structures that are suitable only for a set of vehicle components in which maximizing the energy absorption or minimizing the intrusion is the main concern. However, there are some other components in a vehicle structure that should have characteristics of both stiffness and flexibility. Moreover, the load paths within the structure and potential buckle modes also play an important role in efficient functioning of such components. For example, the front bumper, side frame rails, steering column, and occupant protection devices like the knee bolster should all exhibit controlled deformation and collapse behavior.

This investigation introduces a methodology to design dynamically crushed thin-walled tubular structures for crashworthiness applications. Due to their low cost, high

energy absorption efficiency, and capacity to withstand long strokes, thin-walled tubular structures are extensively used in the automotive industry. Tubular structures subjected to impact loading may undergo three modes of deformation: progressive crushing/buckling, dynamic plastic buckling, and global bending or Euler-type buckling. Of these, progressive buckling is the most desirable mode of collapse because it leads to a desirable deformation characteristic, low peak reaction force, and higher energy absorption efficiency. Progressive buckling is generally observed under pure axial loading; however, during an actual crash event, tubular structures are often subjected to oblique impact loads in which Euler-type buckling is the dominating mode of deformation. This undesired behavior severely reduces the energy absorption capability of the tubular structure. The design methodology presented in this paper relies on the ability of a compliant mechanism to transfer displacement and/or force from an input to desired output port locations. The suitable output port locations are utilized to enforce desired buckle zones, mitigating the natural Euler-type buckling effect. The problem addressed in this investigation is to find the thickness distribution of a thin-walled structure and the output port locations that maximizes the energy absorption while maintaining the peak reaction force at a prescribed limit. The underlying design for thickness distribution follows a uniform mutual potential energy density under a dynamic impact event. Nonlinear explicit finite element code LS-DYNA is used to simulate tubular structures under crash loading. Biologically inspired hybrid cellular automaton (HCA) method is used to drive the design process. Results are demonstrated on long straight and S-rail tubes subject to oblique loading, achieving progressive crushing in most cases.

CHAPTER 1. INTRODUCTION

1.1 Automotive Safety

Automobile accidents cause death of about 1.3 million people every year all over the world. The various factors contributing to the death toll are alcohol, vehicle speeding, behavior of the driver, road environment and the vehicle type. Preventive measures that have been taken to reduce injuries by enhancement in the vehicle design to make it crashworthy, improving traffic control and by road improvements. Although, these measures have reduced injuries to some extent, recent study shows that improvement in the design of the vehicle has played an important role in the decline of the death rate.

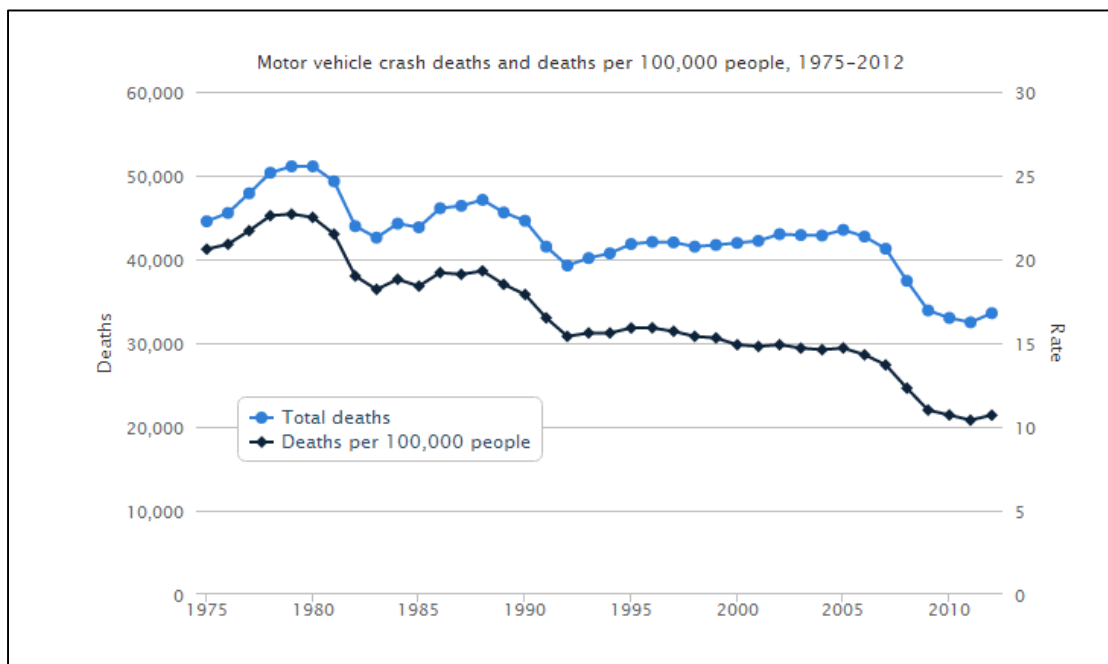


Figure 1-1: Motor vehicle crash deaths per 100,000 people by type, 1975-2012

Figure 1-1 is based on the analysis of data from the US Department of Transportation's Fatality Analysis Reporting System (FARS) [1, 2]. In 1975, the total number of deaths occurred was 44,525 whereas death rate (deaths per million) occurred was 20.6. In 2012, the total number of deaths occurred was 33,561 whereas the death rate was 10.7. The death rate reduced by half and the total deaths by around 20,000 from 1975 to 2012. This is possibly due to various improvements over the years in terms of the road quality, vehicle design and medical facilities. Figure 1-2 shows the graph of driver deaths per hundred thousand registered vehicles. It shows a comparison between the actual death rate vs a hypothetical death rate considering the vehicle design did not change from 1985. In 2004, there could have been 5200 more lives lost only in US [3]. This facts, certainly prove that the decline in the death rates is due to safer and crashworthy vehicles and not better drivers or improved roads.

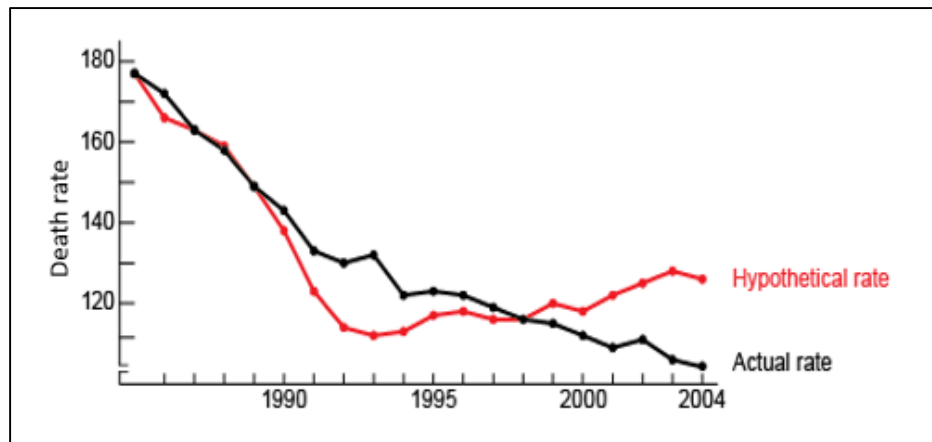


Figure 1-2 : Influence of Vehicle Design Improvements: Driver deaths per hundred thousand registered vehicles, actual death rates vs. hypothetical death rates based on 1985 vehicle design.

This study reveals that over the past couple of decades there are two factors that influenced the driver's death rate. One is the vehicle use patterns change as the vehicles ages, and the other is the vehicle design, replacement of the unsafe vehicles with a more crashworthy ones. As vehicles age, the death rate goes up. On the other hand, more crashworthy vehicles have been introduced and their death rates are lower than the older vehicles they replaced. Hence, there is a need to continue improvement of the vehicles as it is the main protection in crashes with unchecked driving behavior like speeding and traffic policies.

1.2 Crashworthiness

In the early 1950s the term 'crashworthiness' was first used in the aviation industry to investigate the limits of human tolerance. It provided a measure of the ability of a structure/component to protect the occupants in any survivable crashes. Similarly, in the automotive industry crashworthiness pertains to the ability of the structure or any of its components to protect a passenger of a vehicle by resisting the effects of an impact under in the event of collision.

Vehicle crashworthiness and passenger safety are the most important and challenging design considerations. There has been a huge evolution over the past years till present due to the various vehicle types and hence in the goals and requirements of crashworthiness. Current vehicles have bodies manufactured using stamped steel panels and are assembled using various techniques. Designers create vehicle structures basically to provide occupant safety by maintaining the integrity of the passenger cabin while simultaneously controlling the crash deceleration pulse to fall below human survivable levels. Therefore, the goal of

crashworthiness is an optimized vehicle structure that can absorb significant crash energy by controlling deformations while maintaining adequate space so that residual energy can be managed by the vehicle restraint system to minimize crash loads transferred to the occupants.

Considering real time scenarios there could be distinct events of vehicle collisions of similar or different types, sizes, stiffness, masses or shapes. It could also be with a stationary object such as a tree, building, bridge or utility pole. Single and multiple impacts also come into picture while classification. For the purpose of body development safety experts classify vehicle collisions as frontal, rear, side or rollover crashes. Moreover, a vehicle crashes over a wide range of speeds. Keeping these scenarios in mind designer's work on the body development of the vehicle to satisfy the crashworthiness.

The methods like accident reconstruction or analysis of vehicle crash analysis do not provide quantitative information necessary for the vehicle design such as deceleration pulse, occupant kinematics or loads, passenger safety. Vehicle crashworthiness is evaluated in four different modes: frontal, rear, side and rollover crashes. Hence, design engineers rely on the standard laboratory test combined with ground evaluations and analysis to achieve safety of the occupant.

1.2.1 Controlled Energy Absorption for Crashworthiness Design

Energy absorption being the most important characteristic of a crashworthy component, it is also vital to have a controlled energy absorption design. For example, the front structure of a vehicle should be stiff, yet deformable, with crush zones to absorb crash energy resulting from frontal impacts through plastic deformation and to prevent severe

intrusion into the passenger cabin. In other words, the structure should exhibit characteristics of both stiffness and flexibility. The optimization problem formulation must accommodate conflicting criteria such as a maximum acceleration or peak contact force constraint to avoid driver and passenger injuries due to too high forces and a maximum deformation constraint to avoid passenger and driver injuries due to penetration of the passenger cabin [4]. A structure with a constant high contact force (just below the injury criteria) throughout the crash event satisfies these requirements in the best manner.

A structure is required to follow a prescribed force-displacement history for ideal operation under crash. Apart from controlling peak contact force and maximum intrusion, other factors like load carrying paths, relative stiffness and potential buckle modes within the crashworthy structure are also important to consider while designing for specific purposes. A structure can absorb the same amount of energy under a high peak force with low intrusion or a low peak force with high intrusion. A structure with high peak force would be a stiffer structure and low peak force with high intrusion more flexible structure. However depending on the specific purpose the crashworthiness design has to be chosen to have a controlled energy absorption or controlled deformation characteristic.

1.2.2 Automotive Crashworthiness Requirements for a Body in Prime (BIP)

Every component in the vehicle body has a specific requirements of crashworthiness. There are certain requirements for the component of the vehicle structure to yield a satisfactory deceleration for a range of crash speeds and occupant sizes .These are stated as follows:

- 1) Stiff yet deformable frontal structure with crush zones to absorb crash kinetic energy resulting from frontal collisions by plastic deformation and prevent intrusion into the occupant compartment, especially in case of offset crashes and collision with narrow objects like trees. As seen in Figure 1-3 the components of the vehicle structure front bumper beam and part of the frame rails, which prevent severe intrusion in the engine hood and passenger compartment.
- 2) The rear structure to maintain integrity of the rear passenger compartment and protect the fuel tank.
- 3) Appropriately designed side structures to minimize intrusion in side impact and prevent doors from opening due to crash loads.
- 4) Rollover collision protection can be taken care by having a strong roof structure.
- 5) Properly designed restraint systems to provide the occupant with optimal ride down and protect in interior trims and spaces.

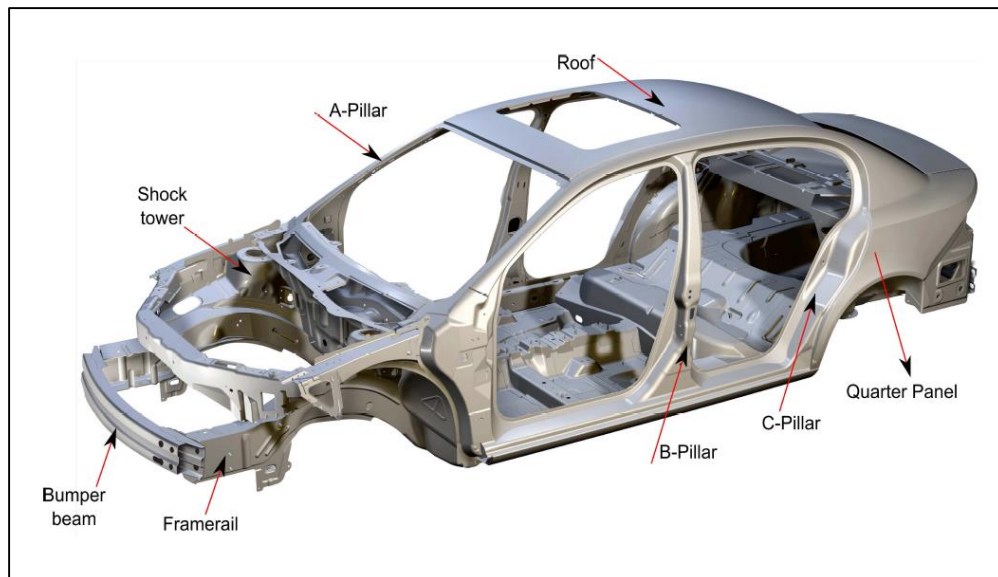


Figure 1-3: Body in white (BIW) structure of a Car

1.2.3 Design for Crashworthiness

The primary tool for evaluating concepts in crashworthiness design was physical experimentation due to lack of computational power in early 1960's. The high costs and long production times eventually led to the development of advanced simulation tools. Due to the advent of Computer Aided Engineering (CAE) tools such as Finite Element method (FEM), helped in the reduction of design time and costs while improving safety and durability of the final product. The design verification is now done using computer simulations which were previously done using prototype testing. This has been possible due to the ability of CAE tools which are designed to predict the actual responses. As the design of crashworthy structures is complex the main aim is to maximize the energy absorbed by the structure during a crash event while ensuring some level of safety at minimum cost. Safety is proportional to the accelerations and forces generated during the crash and the cost is determined by the amount of material required to manufacture the component of the vehicle structure. Crash simulations typically require from hours to days to execute. Most commonly used mechanisms are good engineering judgment and the trial and error to generate designs that exhibit good energy absorption characteristics while maintaining the safety of the occupant. The outcome of these manual mechanisms is not optimal or the best, hence needs to be revisited and amended by using optimization techniques leading to better designs. Methods employed are such as those used in the commercial package LS-OPT, utilize the response surface methodology (RSM) to approximate the design space. RSM is a method used to construct smooth approximations of functions. There has to be an initial structure before application of this methodology, hence considerable effort is required. The ultimate goal of the research is to develop a

methodology to generate an optimal solution for a given crashworthy design problem without the need of any dependency on initial candidate design. This is where topology optimization comes into picture which is used to accomplish this.

Concept designs from the process can be used for achieving crashworthiness considering the increasing demand of vehicles to satisfy the safety regulations, fuel economy, cost of manufacturing and reduction in design cycle time.

1.2.4 Tubular Structures for Crashworthiness

In Automobile, tubular structures are commonly used in the body in white (BIW) structure refer to Figure 1-4. S-Rail which is attached to the front bumper is one of the classic example, refer Figure 1-5. During a crash event the S-Rails act as an energy absorbing components to avoid high impact force, absorb maximum energy and avoid penetration.

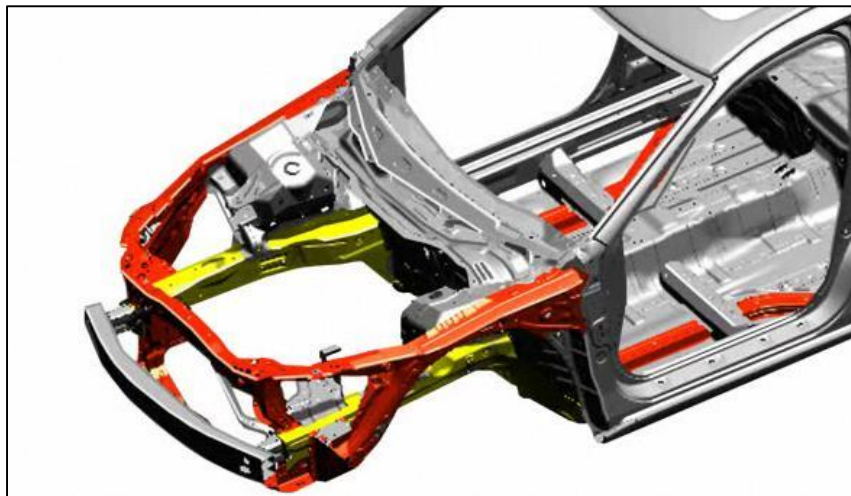


Figure 1-4: BIW structure showing S-Rail

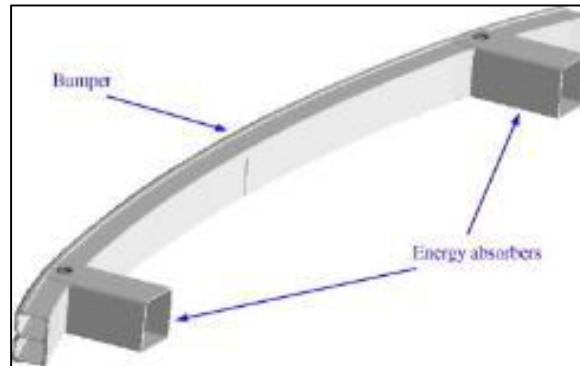


Figure 1-5 Energy absorbers to the bumper.

Thin-walled tubular components are extensively used as structural members in the majority of transportation vehicles because of their low cost, good energy absorption capability and relatively low density. They have the ability to absorb the kinetic energy of the impacting body in the form of plastic deformations, hence protecting the structure and passengers involved. These structures can be used in various loading conditions such as axial crushing, bending, oblique impact, transverse loading, among others. Tubular structures show significant energy absorption for long strokes in an axial crushing mode and hence, present an attractive option in crashworthiness designs. A great deal of research has been done to study the axial crushing of thin-walled tubes since the pioneering work of Pugsley [5] and Alexander [6] in the 1960s. Later work from Abramowicz and Jones on both the static and dynamic responses of tubes focused on theoretical and experimental studies [7-10]. The concept of a superfolding element was introduced by Wierzbicki and Abramowicz [11] to better understand the mechanics of the crushing of thin-walled structures.

Various experimental and numerical studies revealed three dominant modes of deformation during the axial crushing of thin-walled structures: progressive buckling, global or Euler-type buckling, and dynamic plastic buckling [12]. Of these three, the progressive buckling mode is desired for crashworthy designs because of its efficient energy absorption and better force-displacement behavior. In progressive buckling, crushing starting at one end (often the end close to the impact) and progressing systematically toward the other end of the structure is preferred as it utilizes the maximum possible material for plastic deformation without jamming. Figure 1-6 and Figure 1-7 shows a result from the experimental investigations on the behavior of short to long square aluminum tubes subjected to axial loading [13]. A uniform tube when buckles in a progressive manner it shows a desirable force-displacement graph with a lower peak force and higher energy absorbed. A tube when has Euler-type buckling the peak force is high and energy absorbed is less. The change in the impact force being too high makes it undesirable from safety prospective.

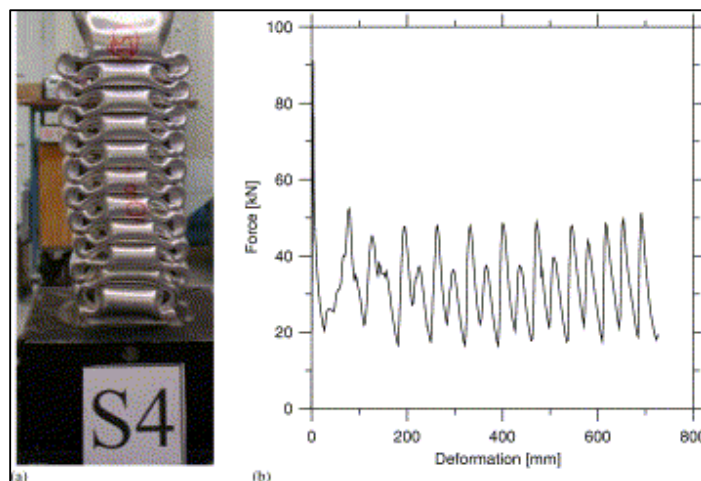


Figure 1-6: Progressive Buckling

It is desired to have these tubular structures to show progressive buckling when subjected to axial or even oblique loading conditions. This need has been addressed in this research and a design methodology is developed to design thin walled tubular structures for crashworthiness.

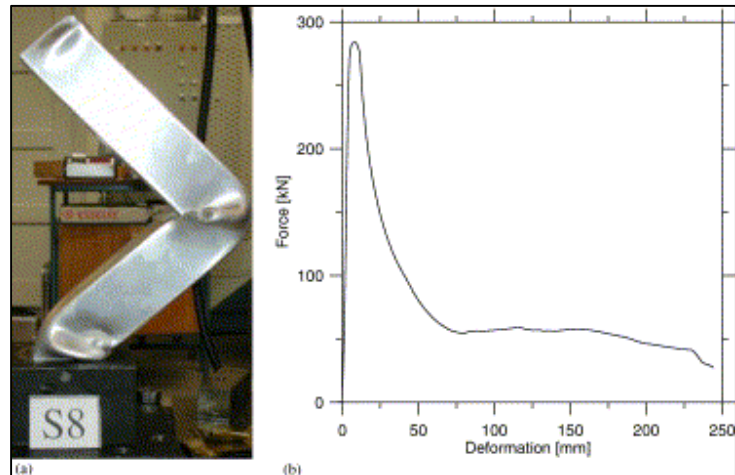


Figure 1-7: Euler-type buckling

1.3 State of the Art

1.3.1 Structural Optimization

The main aim of structural optimization is to obtain optimal mechanical performance at reduced mass. The mass of the structure is proportional to the cost, hence it is ideally expected to have lowest mass possible for the engineering applications. Earlier work was based more on analytical methods searching for optimal configurations using the mathematical theory of calculus and variational methods [14, 15]. With the past two

decades the focus has changed to numerical methods due to advance computational resources and the need to solve complex problems. Numerical methods generate optimal designs in an iterative fashion using finite element analysis and mathematical programming [16-23]. In 1988, this computational method for the optimal distribution of material of continuum structures was first introduced by Bendsoe and Kikuchi [24]. Primarily, there are three approaches to structural optimization techniques such as sizing, shape and topology optimization. Topology optimization can be defined as an iterative process that determines the best arrangement of a limited volume of structural material within a given spatial domain so as to obtain an optimal mechanical performance of the concept design [25-27]. Optimization technique eliminates and redistributes material throughout the domain to minimize or maximize a specified objective. Sizing or parameter optimization generally used cross-sectional properties, such as diameter of a truss member or plate thickness as design variables. Shape optimization is complicated as the design variables used are co-ordinates of the boundary or surface of the structure. Shape optimization is used as a second phase of design after utilizing topology optimization. The design variable thickness is utilized for this research, as it is the variable which is an essential parameter used for element by element topology sizing optimization (also referred as topometry optimization).

Various methodologies have been developed for structural optimization over the past two decades. Most of the existing topology optimization algorithms fall into the categories of mathematical programming (MP), optimality criteria (OC), and evolutionary programming methods [27]. To solve the topology optimization problem, any nonlinear MP method may be used. Sequential Linear Programming (SLP) is an example that

searches for the minimum in a nonlinear design space using a sequence of linear approximations for both the objective and constraints. Similarly, Sequential Quadratic Programming (SQP) methods approximate the objective and constraints with quadratic functions. The Method of Moving Asymptotes (MMA) developed by Svanberg [28] is another widely used MP method for topology optimization. It is similar in nature to SLP and SQP in the sense that it works with a sequence of simpler approximate subproblems of a given type. These methods are usually robust and can be applied to any sort of optimization problem. However, when applied to topology optimization problems, several calculations of the objective function, constraint functions and their derivatives are usually needed [15, 29]. Consequently, the use of mathematical programming methods for realistic topology optimization problems is somewhat impractical, as they usually require thousands of finite elements and therefore, thousands of design variables [30]. OC methods derive or state conditions that characterize the optimum design, then find or change the design to satisfy those conditions while indirectly optimizing the structure. Fully stressed designs (FSD), constant internal force distribution designs (CIFDD), simultaneous failure mode designs (SFMD), and uniform strain energy density designs (USED) are examples of heuristic optimality criteria methods. The use of OC methods for continuum design problems in topology optimization dates back to the pioneering work of Bendsøe and Kikuchi [24].

In contrast to the above mentioned methods, various topology optimization methods have been developed using evolutionary strategies that do not require gradient (sensitivity) information. An often used but less efficient approach is to use genetic algorithms (GAs). These methods are more likely to find the global optimum but require

thousands of function evaluations. Another non-gradient based methodology developed by Xie and Stevens [31] is called Evolutionary Structural Optimization (ESO). In this method, inefficient material is progressively removed from the structure so that it evolves into an optimal design. Another approach developed by Tovar [32] and Tovar et al. [33, 34] that is inspired by the biological process of bone remodeling is known as the Hybrid Cellular Automaton (HCA) method. This method is used as the basic framework for the present work.

Structural optimization for crashworthiness:

Various methods have been introduced by researchers for the use of structural optimization for crashworthiness [35, 36]. Pedersen [37, 38] later devised a method for topology optimization using 2D frame structures. In that work, the objective was to obtain a desired energy absorption history for a crushed structure. The formulation used numerically approximate computed sensitivities. Although this sensitivity-based method was shown to work well for ground structures made of beam elements, it has never been extended to more realistic continuum-element-based structures. Sensitivity-based methods, although more accurate, are not always preferred in topology optimization for crashworthiness design due to: a) the inability to express sensitivities in closed form analytical expressions and b) the large number of design variables.

In order to tackle topology optimization for crashworthiness design of more realistic continuum-element-based components with a significant number of design variables, many heuristic methods have been proposed. Soto [39, 40] presented a methodology that does not require sensitivity information. In this heuristic scheme, Soto

implements a criterion called prescribed plastic strain/stress (PPSS). The PPSS criterion varies the density within the design domain to achieve a prescribed distribution of plastic strains and stresses with a constraint on mass. This methodology utilizes a density approach with two base materials, one that is stiff and one extremely soft, to represent a metallic foam-like material. This method cannot generate solid metal structures. Forsberg and Nilsson [41] proposed another non-gradient technique using thickness as the design variable. However, by operating on the thickness of elements, this methodology can only handle a small set of problems. Patel et al. [42] developed the HCA method, originally proposed by Tovar et al. [32-34], to address crashworthiness design problems. The HCA method for crashworthiness design uses a concept similar to the fully stressed design [15] in which material is distributed within the design domain to achieve uniform strain energy distribution. In the present work, the HCA method for crashworthiness design has been incorporated using a compliant mechanism approach where the material is distributed in the form of thickness to achieve uniform mutual potential energy.

1.3.2 Crashworthy Thin-Walled Tubular Structures

Various design methods have been proposed to improve the design of thin-walled tubes under axial crush loads. These investigations have been aimed to improve the collapse mode and reduce the initial peak force on the tube.

1.3.2.1 Crush Initiators

To achieve good crashworthy designs for thin walled tubular structure designers have evaluated the use of crush initiators. Crush initiators, also known as triggers, stress concentrators, or imperfections, can be used to 1) initiate a specific axial collapse mode, 2) stabilize the collapse process, and 3) reduce the peak force during the axial crush. Many researchers came up with ideas for introducing buckle initiators or surface patterns to enhance energy absorption and buckling behavior [43]. Crush zones in the structure have been used to enforce progressive buckling [44]. Chamfering and other triggering mechanisms have been investigated on quasi-static axial crush of square aluminum tubes [45]. The effect of triggering dents on the energy absorption capacity of axially compressed aluminum tubes has been also investigated [46]. Eren [47] portrayed the use of various crush initiators that can reduce the maximum crushing force and how they affect the observed folding form. Few of those can be seen in the Figure 1-8. Abah et al. [48] investigated the effect of corner cutouts to initiate collapse and reduce the peak load of rectangular tubes under an axial load. Lee et al. [46] introduced triggering dents and investigated the effect of two types of dents, full- and half-dents, with the aim of decreasing the peak load. Shakeri et al. [49] introduced plastic buckling modes as an initial geometric imperfection in the post- buckling analysis to encourage progressive crushing and reduce maximum crush force in cylindrical tubes. Daneshi and Hosseinipour [50] showed that cutting circumferential grooves alternatively inside and outside of the tube at predetermined intervals could be an effective tool to force the plastic deformation to form at predetermined intervals along the tube. Using this pattern, it was possible to control the collapse shape of thin-walled structures.

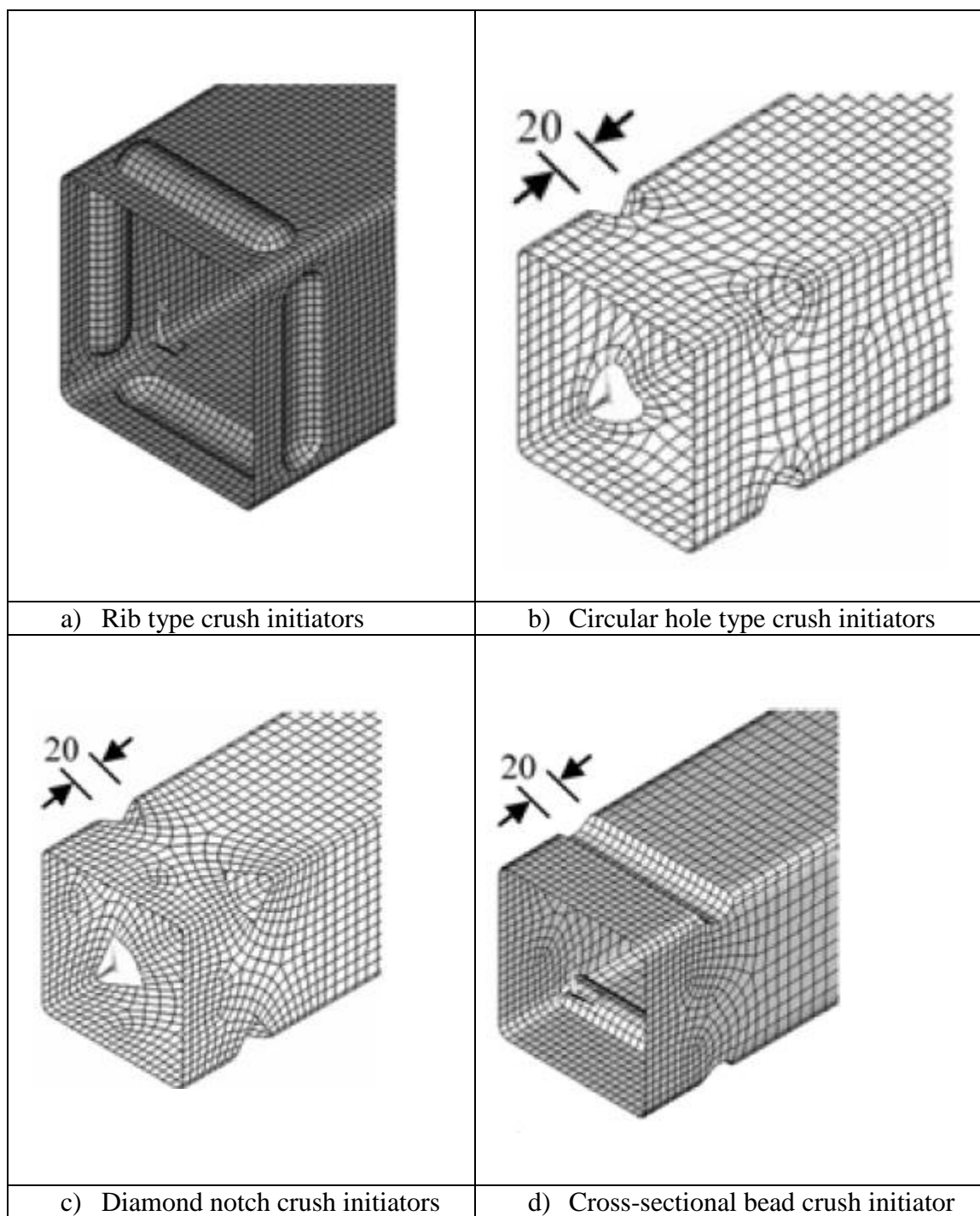


Figure 1-8: Various crush initiators

1.3.2.2 Tapered and Internal Cellular Structures

Nagel and Thambiratnam [51-53] compared the energy absorption of straight and tapered thin-walled rectangular tubes under quasi-static and dynamic axial as well as off-axial dynamic impact loading. They showed the advantages of using tapered tubes for energy absorption under oblique impact loading. The energy absorption and load-bearing capacity under axial compression of some model cellular structures were studied. Chai [54] considered three configurations cellular based designs: multilayer, multi-cell and multi-tube, all of a rectangular-cell topology.

1.3.2.3 Foam Filled Structures

The foam filled thin-walled structures have more recently become an increasing area of research due to rapid development of various filler materials and understanding of their special features in energy absorption. Internal stiffening of metallic tubes with filler materials such as wood, metallic or non-metallic honeycomb and foam have shown to improve an energy absorption capacity in a number of investigations [55-57]. Non-compact crushing and global buckling behavior under axial loads are eliminated in the foam-filled tubes. Moreover in comparison with empty tubes of the same size, foam-filled tubes are less affected by loading parameters (i.e., direction and uniformity) and are more stable during the collapse process. For example, Zhang and Cheng [58] conducted a comparative study of energy absorption characteristics between foam-filled square columns and multi-cell square columns by using nonlinear finite element code. Mirfendereski et al. [59] also compared the energy absorption behaviors of empty and foam-filled tapered thin-walled

rectangular tubes under the quasi-static and dynamic crush loading. Zarei and Kroger [60, 61] optimized the energy absorption characteristic of straight empty and foam filled square aluminum tubes. Ahmad et al. [62] investigated dynamic energy absorption characteristics of foam-filled conical tubes under oblique impact loading.

1.3.2.4 Design Methodology for Crashworthy Tubular Components

Different design methodologies have been introduced by the researchers for the design of crashworthy thin walled tubular structures. Salehghaffari et al. [63] introduced a design concept by machining wide circumferential grooves from the outer surface of a thick-walled tube at specific intervals, they arrived at a general design concept for an integrally stiffened (monolithic) tube. The thicker portions (rings) essentially act as external stiffeners for the enclosed thin-walled tube sections. When the stiffened tube is subjected to an axial compression, the thin-walled sections between two adjacent ring stiffeners fold resulting in an enhanced energy absorption. Designers have incorporated optimization of tapered thin walled structures [64, 65]. To address the shortcoming of uniform density foam fillers, researchers have incorporated functionally graded foam fillers, which contain continuously varying cells in a predefined manner [66]. Functionally graded foam-filled tapered tube was studied by Yin et al. [67, 68]. Using the metamodel techniques for the foam-filled multi-cell thin-walled structures, designer finds the density in each segment that maximizes the specific energy absorption and minimizes the peak crushing force [69]. The results demonstrate improved energy absorption and progressive folding than traditional uniform density foam fillers.

1.3.2.5 What is Missing?

Effectiveness of most of the designs largely depends on the direction of the load and the general shape of the component. Most of the designs are tested on axisymmetric, straight components under axial impact, but their effect on irregular geometries under oblique impact is less evident. The tapered structures being axisymmetric makes it more appropriate for benchmark studies. The use of uniform high-density aluminum foam may reduce specific energy absorption [70] and promote Euler-type buckling under axial and oblique impact [62, 71]. Most of the design methodologies have their design performance highly depends on the geometry and the number the segments.

There are no methods to assist the designer in conceptualizing this design. Here in this research we introduce a topometry based design methodology which would help the designer conceptualize the design.

1.4 Research Objective

The overall objective of this research is to develop crashworthy structures with controlled behavior. We begin the research with the implementation of the hybrid cellular automaton (HCA) synthesis for the design of crashworthy structures. However, the main focus is on the design methodology developed for the design the thin walled tubular structures used for crashworthiness. This methodology has been demonstrated for the structures with geometric implementation with oblique loading and on a complex geometry of S-Rail.

1.4.1 Numerical Implementation of a Structural Synthesis Method for Crashworthiness

The hybrid cellular automaton (HCA) method is a computational technique that can be used to synthesize optimal topologies. This approach is inspired by the biological process of bone remodeling developed by Tovar [34]. HCA was incorporated to design the crashworthy structures. Numerical examples were solved to demonstrate the application of the HCA synthesis. Chapter 2 demonstrates the implementation of HCA and its numerical implementation. A topology optimization problem is solved for a bumper like structure subjected to crash and helped improve the energy absorption capabilities and mass reduction. Further topography optimization is performed on a flat plate subjected to impact to reduce the penetration on the structure. HCA was then implemented to achieve the compliant mechanism design using a force inverter example which is demonstrated in 2.3.3.

1.4.2 Structural Synthesis of Thin-Walled Tubular Components

Most of the energy-absorbing structures often take the form of thin-walled tubular metallic structures subjected to dynamic compressive loads. Our main focus is to develop a design methodology for the design of such crashworthy thin walled structures. For example, the front frame rails in a vehicle play an important role during frontal collisions by absorbing crash energy through plastic deformation. For efficient energy absorption, these tubular structures should undergo progressive buckling, preferably starting from the loading end to ensure maximal usage of material for plastic deformation. However, the presence of imperfections or asymmetry loading conditions can trigger buckling starting from the middle or even close to the rear end of these structures, leading to possible

jamming or global (Euler-type) bending behavior, which adversely affects the energy absorption capability.

In order to ensure a progressive collapse behavior, preferably starting from the loading end, a new methodology based on compliant mechanism design is presented in this research. The underlying idea is to design the tube to trigger the symmetric mode of collapse near the impact end. Within topometry-based compliant mechanism design, output port definitions on the tube faces along its length create potential buckle zones in the final design. A significant advantage of this method for designing thin-walled tube structures is the possible delay or complete avoidance of global (Euler-type) bending behavior during oblique loadings which otherwise adversely affects the load-carrying and energy absorption capacity of the structure.

We here introduce a design methodology for the design of thin walled tubular structure using a topometry based compliant mechanism approach. Experiments were performed for the tubular structures with geometric imperfection and at an oblique impacts. Further this methodology has been used to show to have its potential application in designing S-rails typically used in automotive chassis.

1.4.3 Proposed Weighted Approach for Thin-Walled Tubular Component Synthesis

By the compliant mechanism approach we design the tube to initiate its buckling at the output port location and we achieve that by making the structure compliant or flexible. However an S-rail which connects the bumper would still need to be stiff enough to sustain low impact crash events. There are additional crash pads in the system so as to resist the lower impact. Moreover these structures will have other functional requirements too where

it need to be stiff enough. There would always be a need of improving the stiffness of the structure. This approach is developed to give us a better control over the stiffness requirements of a structure. Here we propose a design methodology considering a weighted optimization approach so as to minimize the compliance, to increase the stiffness and implement the compliant mechanism to achieve deformation characteristic required for crashworthiness.

1.4.4 Original Contributions

Design of thin walled tubular structures using a topometry based compliant mechanism approach was first introduced by Bandi [72, 73]. In this research we have incorporated the compliant mechanism approach to establish the design methodology for the design of thin walled tubular structures with geometric imperfection subjected to axial and oblique impact. This design methodology was then used to design the automotive S-rail which has more complex geometry. In this research we have introduced a weighted objective approach between a compliant mechanism design formulation and a minimum compliance problem. This approach helped improve the design further to have better control on the initial peak force and to sustain oblique impact at higher impact angles.

CHAPTER 2. NUMERICAL IMPLEMENTATION OF STRUCTURAL SYNTHESIS FOR CRASHWORTHINESS USING HCA

2.1 Structural Optimization

The main objective of structural optimization is to maximize the performance of a structure or structural component. The various factors on which the optimal structural design depends is the limited material resources, environment impacts and technological competition which demand lightweight, low-cost and high-performance structures. Design which minimizes or maximizes a performance objective considering these constraints is considered to be an optimal design. A structural optimization problem can be mathematically expressed as follows:

$$\begin{aligned}
 & \textit{find: } x \\
 & \textit{minimize: } f(x) \\
 & \textit{subject to: } g(x) \leq 0 \\
 & \qquad \qquad \qquad h(x) = 0 \\
 & \qquad \qquad \qquad x_{min} \leq x \leq x_{max}
 \end{aligned}
 \tag{2.1}$$

where $f(x)$ is the objective function to be minimized, x is the set of independent design variables, g is the set of inequality constraints, and h is the set of equality constraints. The design variable values are constrained by lower bound values (x_{min}) and upper bound values

(x_{max}). Depending on the problem formulation and requirements, various structural performance measures like weight, stiffness, critical load, stress, or displacement, among others, form the objective function and constraints. A commonly used optimization formulation is to maximize the stiffness of a structure subject to a mass constraint. As stated before earlier work in topology optimization was generally used for solving small scale problems with assumption of elastic material properties, small deformations and static loading conditions. Topology optimization aims to achieve maximum stiffness or minimum compliance with a constraint on the mass M . This can be mathematically expressed as follows:

$$\begin{aligned}
 & \textit{find:} \quad x \\
 & \textit{minimize:} \quad c(x) \\
 & \textit{subject to:} \quad m(x) \leq M^* \\
 & \quad \quad \quad x_{min} \leq x \leq x_{max}
 \end{aligned}
 \tag{2.2}$$

where x is the design variable (relative density), m is the mass, M^* is the constraint on mass, and x_{min} and x_{max} being the bounds on the design variables. Other objectives and constraints that could be considered are global structural responses such as von Mises stresses, strains, eigen frequencies, and geometrical parameters such as volume or perimeter. Duysinx and Bendsøe [74] and Lipton [75] introduced a constraint based on local stress distribution. With appropriate choices of the objective and constraints, topology optimization has been extended to a wide variety of applications like compliant mechanism design, frequency response optimization, buckling problems, topology optimization over the past two decades. Various methodologies have been developed as a part of this development. The

categorization of the existing topology optimization algorithms is made into mathematical Programming (MP), optimality criteria (OC) and evolutionary programming methods. There is another approach developed by Tovar [76] and Tovar et al. [32, 34, 76] that is inspired by the biological process of bone remodeling is known as the heat conduction, and stokes flow, among others. A comprehensive review of topology optimization can be found in Sigmund and Bendsøe [4], Rozvany [26], Eschenauer and Olhoff [77], and Bendsøe et al. [78].

There have been extensive developments in Hybrid Cellular Automaton (HCA) method. HCA is used as the basic framework for the present work and is discussed in detail further in this chapter.

2.2 Hybrid Cellular Automaton (HCA) Synthesis

The Hybrid Cellular Automaton (HCA) method is a synthesis technique used to facilitate shape and topology optimization. HCA methodology has been developed for application for continuum structures. This approach is inspired by the biological process of bone remodeling as presented by Dr.Tovar (Tovar et al., 2004). Topology optimization is a technique which has been developed for generating optimal structural design concepts. Gradients can be easily calculated by deriving analytically while designing structures where it is assumed that the structure elastically deforms with small deformations and the loads are static. To address the crashworthiness design problems that include plasticity with dynamic loading, the derivation of the gradients analytically is not possible and numerical calculation is impractical due to the large computational cost of the analysis. Taking the advantages into account of the non-gradient methods they are considered to be

ideal. The Hybrid Cellular Automaton (HCA) method is a non-gradient topology optimization method which is developed for linear static design problems. It will be utilized to develop a novel method for use with dynamic problems that involve plastic deformations. Material is appropriated to uniformly distribute the effects of a specialized mechanical stimulus, or field variable throughout the design domain. The HCA method combines the Cellular Automaton (CA) paradigm with Finite Element Analysis (FEA) for structural optimization. The algorithm has been modified to handle shell elements to achieve the purpose of topometry optimization.

2.2.1 Cellular Automata

In Cellular Automata (CA), which is a discrete model studied in compatibility theory and mathematics (Wolfram, 2002) [79] consists of an infinite, regular grid of cells, or lattice, where each cell is characterized by a finite number of states. There could be any number of finite dimensions with discrete time, and the state of each cell at a given time t is a function of the state of a finite number of neighboring cells named neighborhood cells at time t . The function of the states of a finite number of neighboring cells defines the states of each cell at a given time t . There are certain set of rules applied based on the information in its neighborhood. For each generation these set of rules are applied to the entire CA lattice. Relative cells of an individual cell are selected as neighbors and these cells usually do not change. The rule for updating is similar for all cells based on the values in this neighborhood. In late 1940's John von Neumann developed an abstract model of self-reproduction in biology which simulated the cellular automata in the best way. The first CA proposed by Von Neumann was a two-dimensional square lattice composed of several

thousand cells. CA rule made use of the state of each (central) cell in addition to the states of its four nearest neighbors, located directly to the north, south, east, west. Figure 2-1 and Figure 2-2 show some common two and three-dimensional neighborhood layouts.

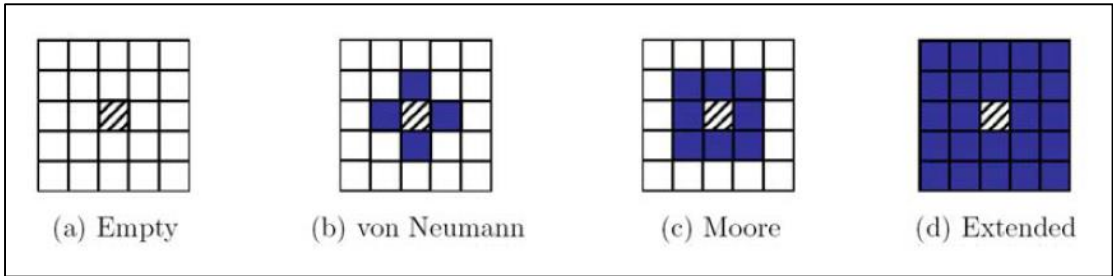


Figure 2-1: Typical 2-D neighborhoods for CA's. N is the number of neighboring CA's: (a) N = 0, (b) N = 4, (c) N = 8, (d) N = 24

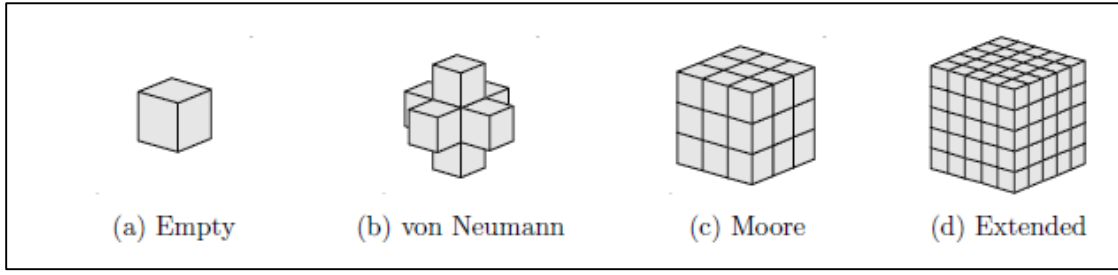


Figure 2-2: The corresponding 3-D neighborhoods for CA's. N is the number of neighboring CA's: (a) N = 0, (b) N = 6, (c) N = 26, (d) N = 124

As discussed earlier in the hybrid cellular automaton (HCA) method, CA paradigm is combined with the finite element analysis (FEA) for structural optimization. The Structural design domain is discretized into material elements in traditional topology optimization methods. In the finite element method for structural analysis, the design domain is represented using the finite element model that is discretized using continuum finite elements (FE). There is a one-to-one correspondence between CA's and FE's which

generally exist but is not a requirement for representing the states of the material elements in the design. For example, mapping a non-uniform FE mesh or a uniform FE mesh with a smaller element size to a uniform CA lattice with a bigger size requires many-to-one FE to CA correspondence. At a discrete position I and time / iteration k , a CA is defined by a set of states that are operated by a set of rules belonging to a given neighborhood of the CA. In CA discretization the uniformity is essential. The state of each CA is defined by design variables x_i (e.g. density, thickness) and field variables S_i (e.g. stress, strain energy density, internal energy density). The field variables are computed by finite element analysis and as each cellular automaton is provided global information HCA is considered as a hybrid approach. The complete state of each cell at time/iteration k is expressed by

$$\beta_i^k = \begin{Bmatrix} S_i^k \\ x_i^k \end{Bmatrix} \quad 2.3$$

The set of local rules operate according to local information collected in the neighborhood N of each cellular automaton. The final state of a CA is defined by the state of itself and the states of the CAs within the neighborhood. For example, the information collected from a neighborhood can be expressed as

$$\overline{S}_i = \frac{\sum_{j \in N_i} S_j}{||N_i||} \quad 2.4$$

where \overline{S}_i is the effective field variable, $N_i = \{j : d(i, j) \leq r\}$, r is the size of the neighborhood, and $||N_i||$ is the cardinal of N_i . A parallel can be drawn between the neighborhood averaging of field variables in HCA and the filtering of sensitivities in traditional topology optimization methods [4] to prevent numerical instabilities of checkerboarding and mesh dependency. In practice, the size of the neighborhood is often

limited to the adjacent cells but can also be extended depending upon the minimum member size requirements.

2.2.2 Design Rules

To obtain an optimal design, material is distributed throughout the design domain in order to achieve a uniform distribution of field variables (actually quasiuniform, as bounds on the design variable restrict the values to achieve full uniformity). Accordingly, a setpoint is uniformly applied to all CAs in the design domain. In the HCA method, the field variable state of each CA is driven to this value. Mathematically, it can be expressed as:

$$\begin{aligned}
 & \textit{find:} \quad x_i \\
 & \textit{minimize:} \quad \sum_{i=1}^N |\bar{S}_i(x_i) - S^*| \\
 & \quad \quad \quad x \\
 & \textit{subject to:} \quad \frac{\sum_{i=1}^N x_i}{N} = M_f^* \\
 & \quad \quad \quad x_{min} \leq x_i \leq x_{max}
 \end{aligned} \tag{2.5}$$

where M_f is the desired mass fraction and a non-zero lower bound of x_{min} is used for the design variable to avoid numerical instabilities due to singular matrices. Adapting the principles of a fully stressed design [15] and uniform strain energy density [80], HCA is utilized to allocate material based on the strain energy density of each element. In other words, strain energy density is used as the field variable to drive the design to an optimal configuration.

Material distribution in the HCA method is governed by control-based rules [33]. These rules manipulate the design variable based on known behavior. Using a proportionality-based control rule, the change in relative density (design variable) of element i at the k th iteration can be expressed as

$$\Delta x_i^k = K_p e_i^k \quad 2.6$$

where K_p is the proportional control gain and e_i is the error between the effective field variable and set point for the i^{th} element. The normalized (scaled) error can be expressed as

$$e_i^k = \frac{\overline{S_i^k} - S_i^{*(k)}}{\|(|\overline{S_i^k}|)\|} \quad 2.7$$

where $\overline{S_i^k}$ is the effective field state of a CA, which reflects the average field state of itself and its neighborhood, and $S_i^{*(k)}$ is the target set point. The equilibrium in a CA is determined by the condition $e_i^k = 0$. When this condition is not satisfied, the local rule modifies the relative density x_i to restore equilibrium. The material is updated from the rule written as

$$x_i^{k+1} = x_i^k + \max\{-\Delta x_{max}, \min(\Delta x_{max}, \Delta x_i^k)\} \quad 2.8$$

A scheme for finding this target is achieved by simply iterating on the HCA update rules and updating the set point until the correct mass results after applying the design rule. The set point update for the $(k + 1)^{\text{th}}$ HCA iteration can be written as:

$$S^{*(k+1)} = S^{*(k)} \left(\frac{M_f^{k+1}}{M_f^*} \right) \quad 2.9$$

where M_f^* is the mass fraction target. The initial set point $S^{*(0)}$ is the average of the field variable of all elements in the design domain for the 0^{th} iteration. When mass of the

structure at the k^{th} iteration satisfies the mass target, the resulting material update control loop is terminated and the dynamic analysis is performed on the resulting material distribution for the $(k + 1)^{\text{th}}$ iteration unless the topology has converged based on the stopping criterion. Thus, the mass constraint is enforced at each HCA iteration.

In an iterative design method, a convergence criterion needs to be defined in order to obtain a final design. Convergence is achieved when the difference between two successive designs becomes less than a user-defined tolerance limit.

To quantify the difference between two designs, the sum of the absolute difference between the design variables is used in this work. Also, in order to avoid premature convergence, three consecutive designs are compared as:

$$\|x^k - x^{k-1}\|_{\infty} + \|x^k - x^{k-1}\|_{\infty} < \epsilon \quad 2.10$$

where ϵ is an arbitrary small tolerance.

So to summarize, the methodology can be represented by the following optimization formulation:

$$\begin{aligned} \textit{find} \quad & x_i && : \text{Design variable} \\ \textit{minimize}_{x} \quad & \sum_{i=0}^N |S_i - S^*| && : \text{Objective - uniform setpoint distribution, e.g., IED} \\ \textit{s. t.} \quad & m_f(x) = M_f^* && : \text{Mass constraint} \\ & x_{min} \leq x \leq x_{max} && : \text{Bounds on design variable} \end{aligned}$$

where $m_f(x)$ denotes the mass fraction of the structure and x_{min} and x_{max} are the bounds on the thickness variable.

2.2.3 HCA Algorithm

The HCA algorithm for topology synthesis of structure under dynamic loading, illustrated in Figure 2-3, is described as follows:

Step 1. Define the design domain, material properties, load conditions and initial design $x^{(0)}$.

Step 2. Evaluate the internal energy density $U^{(k)}$ at each discrete location i using the finite element method (e.g., Ls-Dyna).

Step 3. Update the thickness distribution according to the design rule, to obtain the new design $x^{(k+1)}$.

Step 4. Evaluate the mass of the structure. If the mass target is satisfied, i.e., $|M_f^{k+1} - M_f^*| \leq \epsilon$, proceed; otherwise update the setpoint based on Eq. 2.4 and go to Step 3.

Step 5. Check for global convergence if the convergence criterion is satisfied, the final structure is obtained; otherwise, the iterative process continues from Step 2.

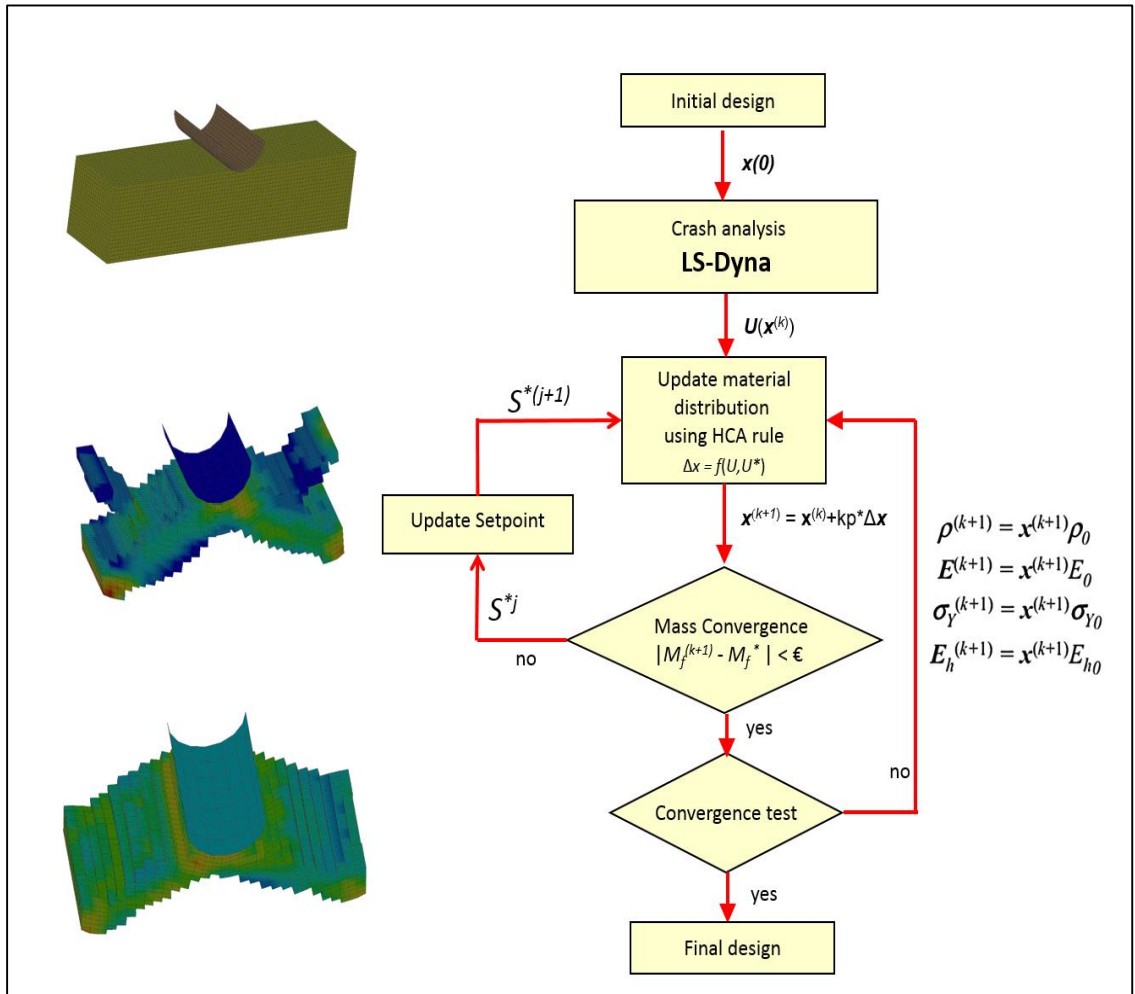


Figure 2-3: Illustration of HCA method for thickness optimization for crashworthiness design.

2.3 Numerical Results

2.3.1 Example 1: Topology Synthesis of a Bumper-Like Structure

As an example a bumper like structure is selected. The initial design or the design space is subjected to an impact from a rigid bar, shown in the Figure 2-4. Such structure

has to absorb maximum energy from the impact and also sustain the impact to avoid penetration. Structures used for car safety like bumper or a side impact bar can be a good example of such a design. LS-Dyna is used to perform the non-linear analysis. The HCA algorithm as discussed in above sections is implemented to obtain the final design.

Internal energy (IE) associated with every element is considered as the field variable and the specific density of every element is the design variable. As the specific density goes below the tolerance or \sim zero the element is removed. The convergence is achieved when the change in design between iterations is below the set tolerance.

From the Figure 2-4 we see the comparison between the initial design and optimized structure. It was clearly evident that the optimized structure has reduced mass and has better energy absorption as compared to the initial design. The final design can be then used as a concept model and developed further to fit the manufacturing constraints.

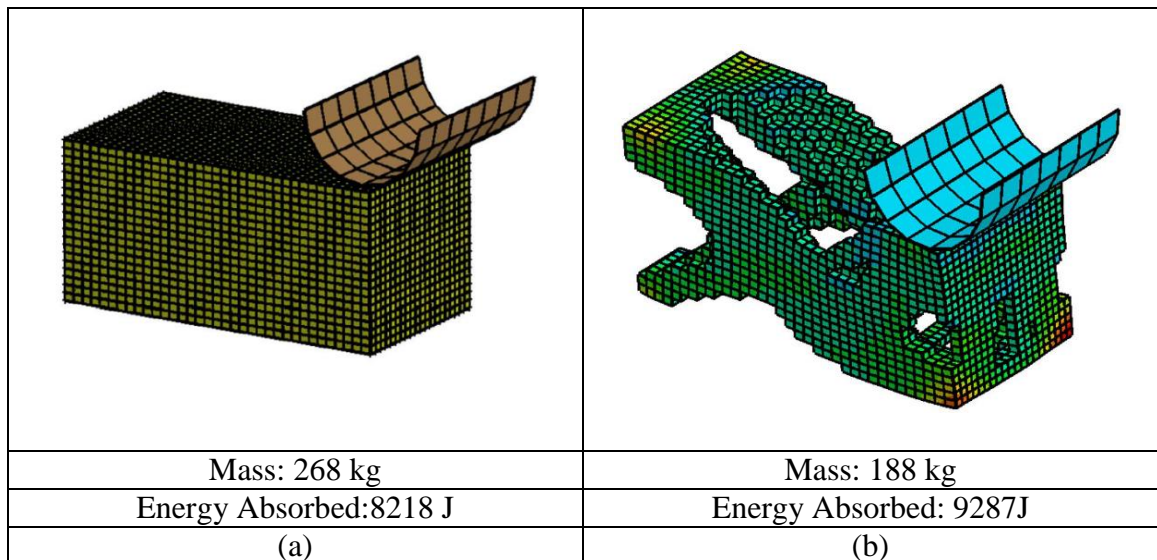


Figure 2-4: Topology optimization of a pumper like structure

2.3.2 Example 2: Topography Optimization of a Base Plate

A base plate was impacted by a ball and the penetration occurred by the impact was measured. Cabin penetration can directly impact the safety of the passengers. Thus the goal of this example was to reduce the penetration due to impact by changing the shape or topography of the plate. Figure 2-5 shows the lower and upper bounds on box constraints given to define the design domain. HCA algorithm was used to solve this problem. The stated example can be seen in the Figure 2-6. Here the field variable used was the displacement at every node and the design variable is the nodal location itself. The converged design is obtained when the design between iterations does not change over a tolerance limit. The final result as illustrated showed a better penetration compared to the initial design. This type of optimization approach can be further extended for the use of sheet metal components in automobile, blast mitigation for army tanks, etc.

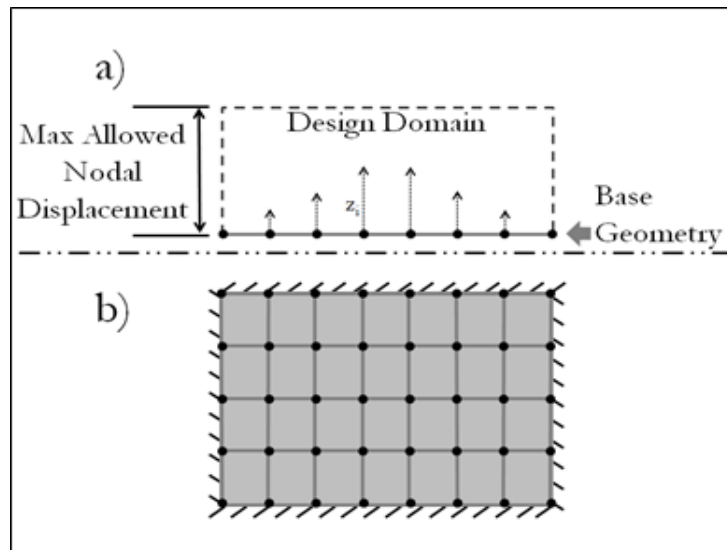


Figure 2-5: Box constraints for the topography design

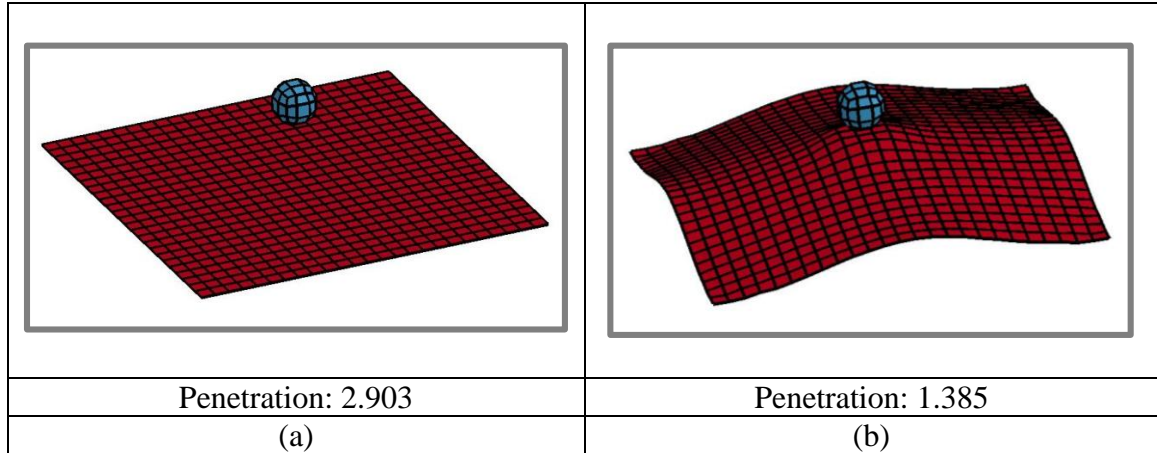


Figure 2-6: Topography optimization of a base plate

2.3.3 Example 3: Force Inverter Design

As an example of a compliant mechanism design problem we will consider the displacement inverter in Figure 2-7. The goal of the topology optimization problem is to design a structure that converts an input displacement on the left edge to a displacement in the opposite direction on the right edge. In order to be able to transfer work from the input port to the output port, the inversion must be performed in a structurally efficient way. Also, it must be possible to control the displacement amplification of the mechanism. The modelling of the input force and displacements should model physical actuators that may have limited strokes, actuation and blocking forces. Assuming that the input actuator is a linear strain based actuator it can be modelled by a spring with stiffness K_{in} and a force F_{in} .

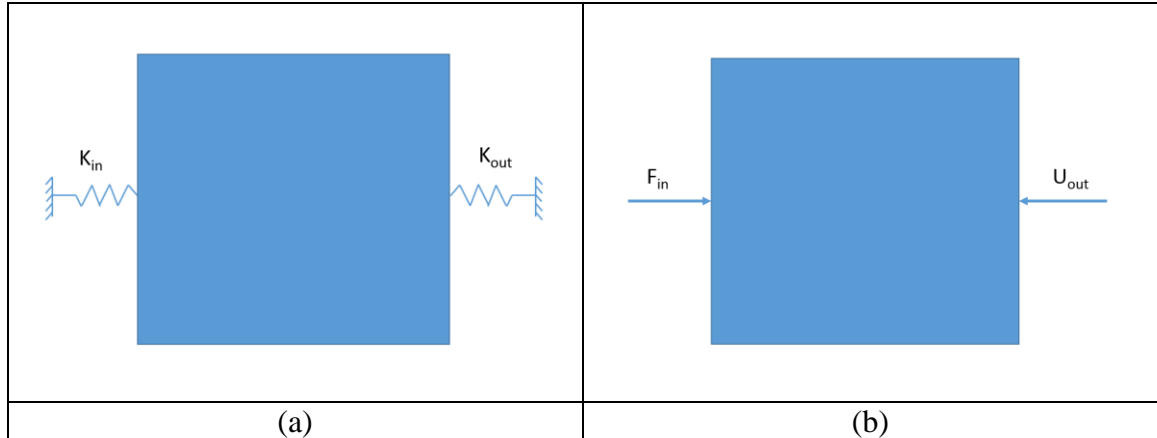


Figure 2-7: Force Inverter Design problem.

The compliant mechanism problem is solved in Matlab using Optimality Criteria by Sigmund in 1997 [81]. Here we have solved the force inverter problem using this established code and compared it with our implementation using the HCA algorithm. The

Figure 2-8 shown the comparison of the results obtained from the Optimality Criteria and Hybrid Cellular Automata. This comparison helps us verify the implementation of HCA algorithm. The implementation of HCA is explained further in the following section. This compliant mechanism approach is then further extended for the design of tubular structures.

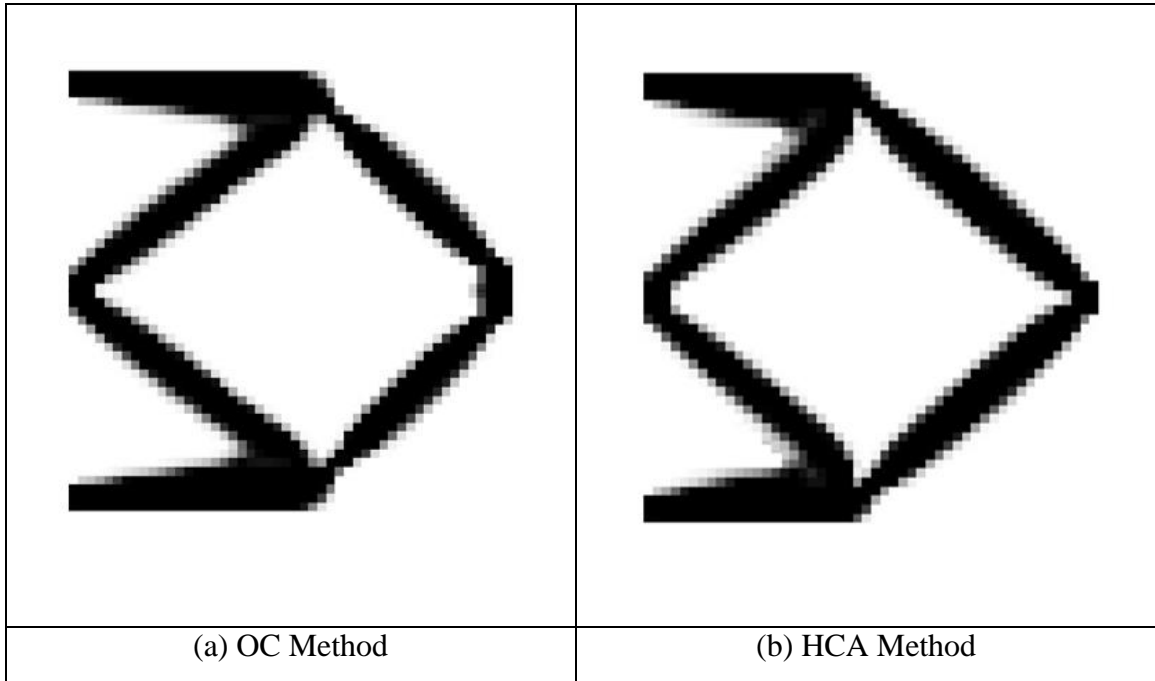


Figure 2-8: Force inverter optimization results.

CHAPTER 3. STRUCTURAL SYNTHESIS OF THIN-WALLED TUBULAR COMPONENTS

3.1 Technical Background

During an actual crash event, the tubular structure will seldom be subjected to pure axial loads. For example, thin-walled structures are subjected to both axial forces and bending moments in an oblique crash. A phenomenon of onset of global bending or Euler-type buckling is observed in thin-walled tubes under oblique impacts if the load angle was higher than a critical value [82, 83]. This onset of global bending severely reduces the energy absorption capability of tube structures. During progressive buckling the maximum peak force F_{max} appears when the buckling starts in the structure for the first time, and after that, the force oscillates between local peaks and minimum loads as shown in Figure 3-1. Each pair of peaks is associated with the development of a wrinkle or buckle. Usually, these wrinkles or buckles develop sequentially from one end of a tube so that the phenomenon is known as progressive buckling. Designers often ignore the oscillations in the force-displacement behavior and use a mean value F_{mean} as an indicator of the energy absorption capability.

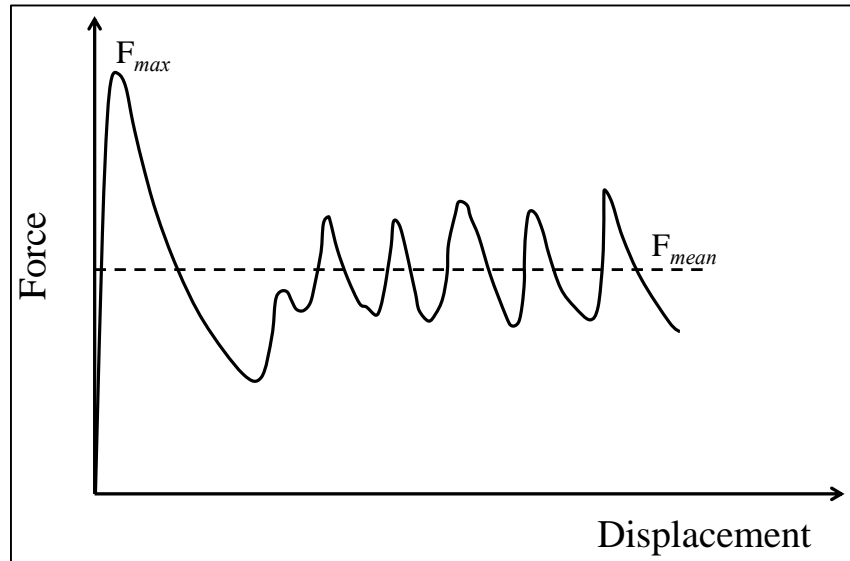


Figure 3-1: Typical force-displacement behavior for an axially crushed thin-walled square tube.

The present work is to design the thin-walled structure in order to invoke a symmetric mode of collapse by defining output ports on the two parallel faces pointing inward. During axial crushing of thin-walled square tubes, it is often desired that the folding or collapse start at the front end (end closer to the impact) and progresses systematically toward the other end of the structure to utilize the maximum possible material for plastic deformation without jamming. Also, the progressive buckling from the front end to the rear end helps in protecting important components close to or behind these energy-absorbing structures. For example, the damage for low intensity (~7-10 mph) frontal impacts in automotive vehicles can be restricted to the bumper-beam and crash-box (hence saving the front frame-rail behind them) if the crash-box collapses progressively without jamming. Thin-walled square tubes, however, do not buckle progressively from the front end to the rear end in all cases. The buckling behavior is dependent on many

factors such as loading conditions, geometry, imperfections and asymmetries in the structure, but most importantly, by the direction of the load. While axial load may trigger progressive buckling, oblique impact may cause Euler-type buckling.

Automotive S-rail deforms like two plastic hinges at the rail curvatures, rotation at the free end and plastic hinge at the fixed end. The normal mode of deformation is as seen in the Figure 3-2 where the S-rail bends at the curvature. This deformation pattern is however not desirable for real time automotive application.

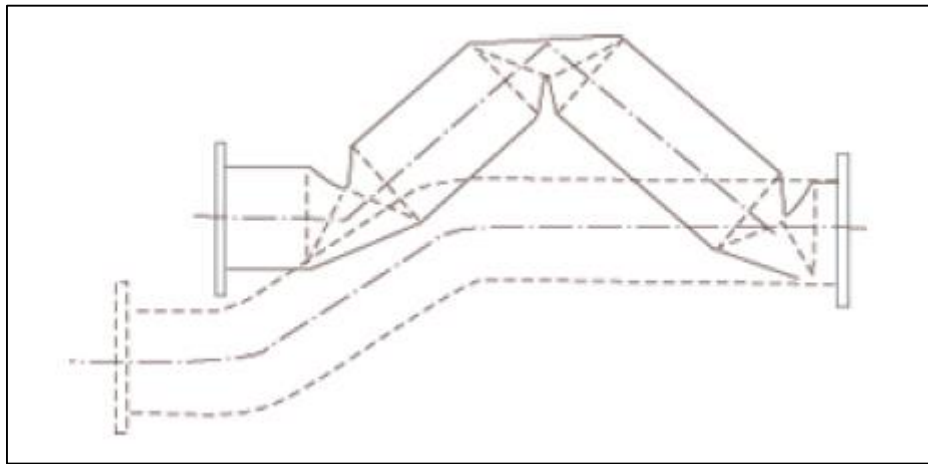


Figure 3-2: Bending mode of collapse for an S-rail

The objective of this work is to define a design methodology to design thin-walled structure such that progressive buckling is achieved even when the structure is having geometric imperfections and is subjected to oblique impact. Later we want to extend this design methodology on to S-Rails, so as to achieve progressive buckling and hence avoiding the S-rails to bend at the curves.

3.2 Proposed Design Methodology

In the methodology presented here, the compliant mechanism design approach is used for thickness-based (topometry) design of thin-walled square tubes under axial compression [84]. The ability of compliant mechanisms to transfer motion and forces from an input load location to the desired points in the structure is utilized to achieve the desired buckle zones in the axial member. By suitably defining the output port locations and desired displacement directions, progressive buckling can be initiated at the desired locations. Moreover, using this method, thin-walled structures can be designed to show progressive buckling even in cases of oblique impact at angles higher than the critical value at which bending collapse dominates the axial collapse and leads to poor energy absorption. To perform thickness-based topometry design of mechanisms, the HCA-based method for compliant mechanism synthesis [85] is modified by using thickness as the design variable. Base line assessment is performed to set benchmark for critical oblique angle and the optimum force-displacement curve. This design problem is approached by following the principles of design of compliant mechanisms. Given the loading conditions, the problem formulation is as follows:

find	thickness distribution
maximize	mutual potential energy
subject to	mass constraint
	thickness bounds
	constitute equations

Compliant mechanism design using topology optimization methods is currently an established approach [86-92]. The use of compliant mechanisms design using topology optimization (material distribution) has been also explored in energy absorbing structural concept design [93, 94]. This work introduces the concept of topometry optimization of

thin-walled structures following compliant mechanism design approaches in order to achieve progressive buckling. The design methodology adopted in this work is described in the following section.

The objective of a compliant mechanism is to efficiently transfer forces and motion from an input actuation location (referred to as input port I/P) to the desired output locations (referred to as output ports O/P) in a structure. Depending on the choice among force, motion or a combination of both to optimize, an appropriate objective function is defined. Geometric advantage (*GA*) is the amplification of the displacement in a mechanism and the mechanical advantage (*MA*) is the amplification of the forces. Alternatively, these objectives of geometric advantage and mechanical advantage can be defined:

$$GA = \frac{d_{out}}{d_{in}} \quad \text{and} \quad MA = \frac{F_{out}}{F_{in}} \quad 3.1$$

where d_{in} and d_{out} represent the displacement at I/P and O/P, respectively, and F_{in} and F_{out} represent the force at I/P and the reaction force at O/P, respectively. In order to obtain such forces, linear springs of stiffness k_{in} and k_{out} are (virtually) attached to I/P and O/P, respectively. Figure 3-3 illustrates the problem's layout. For a given F_{in} the output displacement d_{out} can be determined, from which $F_{out} = k_{out}d_{out}$.

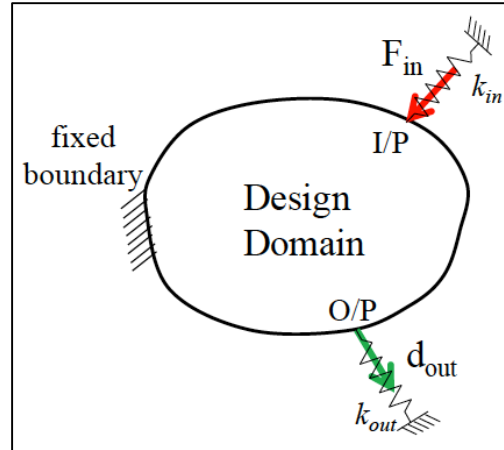


Figure 3-3: Structural optimization set-up in a compliant mechanism design problem using the “dummy load” method.

For a tubular structure, I/P is prescribed at the contact nodes with a rigid wall. The location of O/P corresponds to the desired buckling trigger location. This work proposes that such location may be prescribed according to the designer’s criterion. However, it may be naturally assigned by the wavelength λ of the progressive buckling corresponding to an ideal axial crushing condition (Figure 3-4).

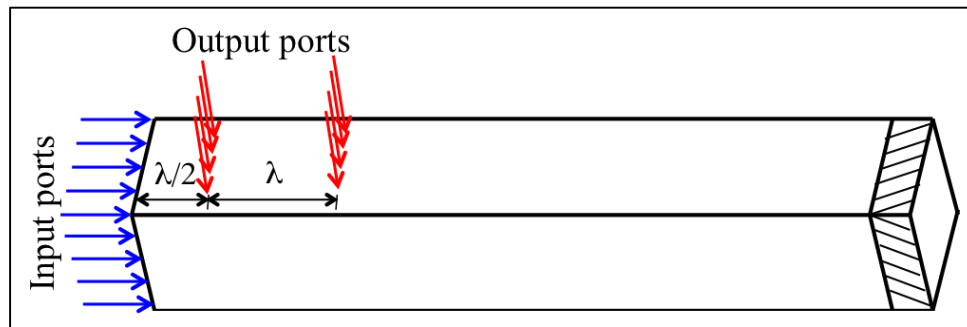


Figure 3-4: Location of input and output ports for a squared tubular structures following the wavelength λ corresponding to the progressive buckling after an ideal axial crushing condition.

For a given input displacement d_{in} , the objective is to maximize d_{out} , i.e., maximize MA . Assuming a fictitious “dummy” unit input force vector \mathbf{F}_d that acts only O/P in the direction of the output displacement, d_{out} can be expressed as the scalar product

$$d_{out} = [0 \cdots 0 \quad 1 \quad 0 \cdots 0] \begin{bmatrix} 0 \\ \vdots \\ d_{out} \\ \vdots \\ 0 \end{bmatrix} = \mathbf{F}_d^T \mathbf{U}_1 \quad 3.2$$

where \mathbf{U}_1 is the displacement vector corresponding to the input load. The product $\mathbf{F}_d^T \mathbf{U}_1$ is termed mutual potential energy MPE or the complementary virtual work [95]. For a discrete finite element model, MPE can be expressed as the sum of element quantities.

$$MPE = \mathbf{F}_d^T \mathbf{U}_1 = \sum_{i=1}^n \boldsymbol{\sigma}_{d_i}^T \boldsymbol{\epsilon}_{1_i} \quad 3.3$$

where $\boldsymbol{\sigma}_{d_i}$ and $\boldsymbol{\epsilon}_{1_i}$ are the element stress and strain vector corresponding to the dummy and the input loads, respectively. The mass M of the structure can be also expressed in terms of element quantities as

$$M = \sum_{i=1}^n \rho A_i t_i \quad 3.4$$

where ρ is the material density and A_i is the area. Nonlinear finite element analysis is required to account for large displacements, contact, and plastic hardening. The two load cases used for the analysis are as shown in the Figure 3-5. Given the crushing loading conditions and the location of I/P and O/P, the design problem can be more clearly expressed as:

$$\begin{aligned}
&\text{Find} && t_i \\
&\text{maximize} && MPE = \sum_{i=1}^n \sigma_{d_i}^T \epsilon_{1_i} \\
&\text{subject to} && M = \sum_{i=1}^n \rho A_i t_i \leq M_{max} \\
&&& t_{min} \leq t_i \leq t_{max} \\
&&& R = 0
\end{aligned} \tag{3.5}$$

where R is the residual in obtaining the structural equilibrium. The input vector load is obtained from the loading condition is used by the optimizer to find the optimum thickness distribution. This corresponds to dynamic event with a given velocity. Sensitivity analysis of geometric nonlinear shell structures under dynamic loading is presented by [35]. Analytical sensitivities for materials nonlinear structures have been considered by [96-98]. Sensitivity analysis for both geometrically and materially nonlinear behavior is reported by [89, 99, 100]. A discussion on geometrically nonlinear material and applications to non-compliant structures and compliant mechanisms is presented by [88, 101]. However, the analytical treatment or numerical approximation of problems involving contact, geometric and material nonlinearities, and dynamic loading conditions, still remains unsolved or intractable. In order to find a solution to the above mention optimization problem, this work incorporates the principles of uniform mutual potential energy distribution using hybrid cellular automata (HCA) [76, 101-104].

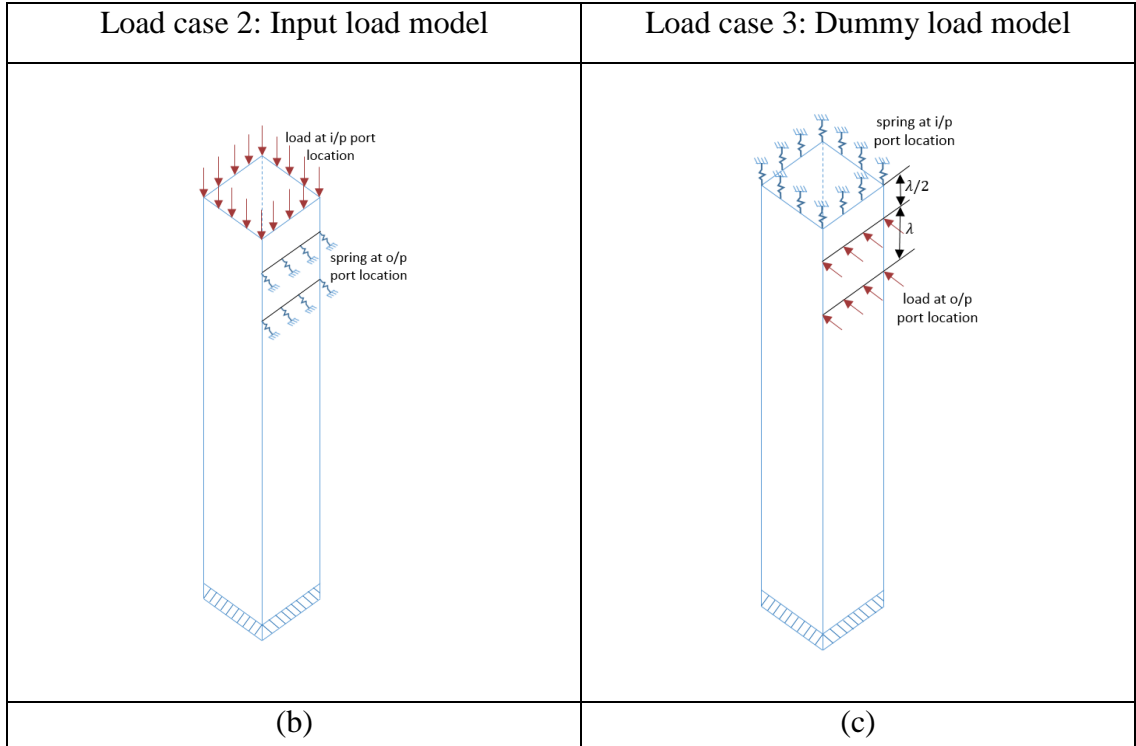


Figure 3-5: Two load cases used for the design methodology.

The hybrid cellular automaton (HCA) algorithm is a structural design methodology inspired by the biological process of bone adaptation [105, 106]. This methodology assumes that cellular automata (CAs) form a structure or design domain, and sensors and actuators within the CAs activate local formation and resorption of material. With a proper control strategy, this process drives the overall structure to an optimal topology by updating the thickness distribution. Using distributed controlled rules, the problem can be restated as:

$$\begin{aligned}
& \text{find} && t_i, \mu \\
& \text{minimize} && |\widetilde{MPE}_i(\mathbf{t}) - MPE^*(\mathbf{t}, \mu)| \\
& \text{subject to} && M = \sum_{i=1}^n \rho A_i t_i \leq M_{max} \\
& && t_{min} \leq t_i \leq t_{max} \\
& && \mathbf{R} = \mathbf{0}
\end{aligned} \tag{3.6}$$

where μ is the Lagrange multiplier associated with the mass constraint. The MPE^* is the target value to be achieved by every element in the structure. This target is a function of the thickness distribution \mathbf{t} and μ . In order to preserve a consistent topology design that is independent of the number of cells, an effective element mutual potential energy \widetilde{MPE}_i defined as a function of the cell's neighborhood size,

$$\widetilde{MPE}_i = \frac{\sum_{j \in N_i} MPE_j}{|N_i|} \tag{3.7}$$

where N_i is the neighborhood of the i -th cell defined by

$$N_i = \{j: d(i, j) \leq r\} \tag{3.8}$$

and $d(i, j)$ denotes the distance between the i -th and the j -th cells. The neighborhood layout depends on the distance r referred to as the range of the neighborhood. Figure 2-1 shows the CA neighborhood layouts for different ranges. The iterative approach may be achieved using a control-based algorithm [76, 107] or a ratio approach [108]. This work makes use of the latter one.

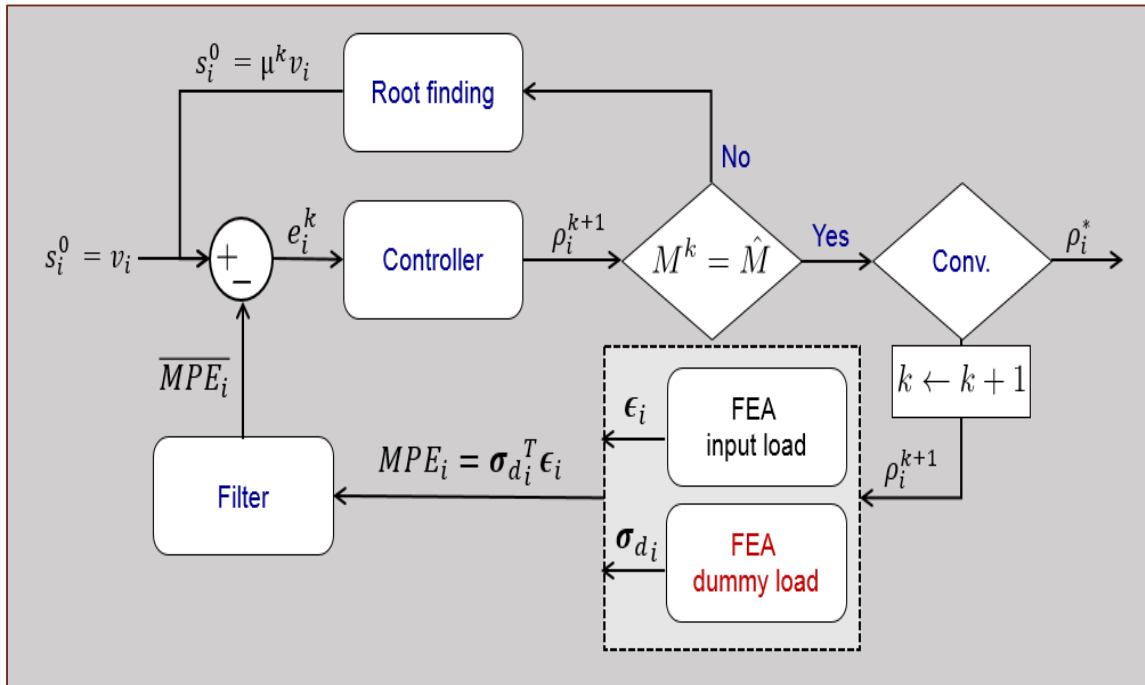


Figure 3-6: Design control algorithm.

3.3 Design Control Algorithm

Design Control algorithm used for the implementation of HCA is shown in the Figure 3-6.

1. s_i^0 is the design variable state at iteration 0 or for base run for the elements $i=1,2..N$.
2. The field variable is calculated for the base run and stored as the set point \overline{MPE}_0 .
As we intend to distribute the MPE equally across the system.
3. For the later iterations ($k = 1, 2 \dots N$) runs the MPE_i^k is calculated from the two FEA load cases.
4. Error e_i^k is computed for every iteration (k), from the set point (\overline{MPE}_0) and the MPE_i^k .

5. This error (e_i^k) is used to update the design ρ_i^{k+1} by using a PID controller as showed in the loop.
6. Mass constraint is verified for every iteration.
7. If mass constraint not met the set point using a bisection method until we meet he constraint.
8. The final design is obtained when the design does not change above the tolerance when compared to its previous runs.

3.4 LS-Dyna Model

Explicit nonlinear finite element code LS-DYNA is used to perform dynamic simulations of axial crushing of square tubes. A linear elastic, piecewise linear plastic material (*MAT24) is used for modeling steel tubes with properties shown in Table 3-1. Generally, thin-walled structures under axial compression are modeled with plane stress shell elements. In several investigations reasonable agreement has been found between shell-based finite element simulations and experimental results [109, 110]. A very efficient plane stress shell element formulation from LS-DYNA (ELFORM=16) that is not subject to hourglassing (spurious strain energy modes) due to 4 in-plane integration points is used to model tubes in this work. Five integration points are used throughout the thickness in order to accurately capture the local element bending. This element is a fully integrated shell with assumed strain interpolants used to alleviate locking and enhance in-plane bending behavior [111].

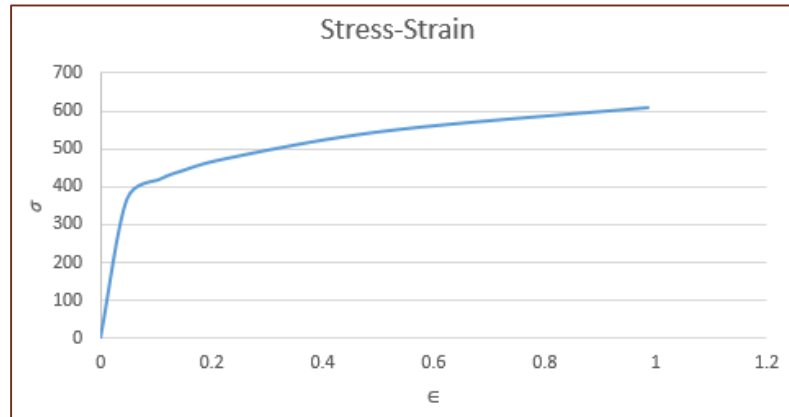


Figure 3-7: Stress-strain curve for the material used for the analysis

Table 3-1: Material properties of steel used for tube models

Property	Value
Density	7800 kg/m ³
Elastic Modulus	207 GPa
Poisson's Ratio	0.29
Yield Stress	253 MPa
Effective plastic Strain	Effective stress (MPa)
0.000	253
0.048	367
0.108	420
0.148	442
0.208	468
0.407	524
0.607	561
0.987	608

The tube is subjected to an impact by a rigid plate with a velocity of 5 m/s axially and then in an oblique angle. Please note the obliqueness in the impact for the entire study has been simulated similar to the practical rig test performed on tubes, so the impact plate is oblique however impact velocity is still axial. The contact between the rigid plate and tube is modeled using a constraint algorithm with a friction coefficient of 0.3 to allow sliding movement. To account for the contact between the lobes (folds) during deformation, a single surface contact algorithm with a coefficient of friction 0.1 is used.

3.5 Numerical Results

3.5.1 Proposed Benchmark Structures

During the practical crash scenario the impact may be at any angle. While designing a structure to sustain such kind of impact, there are geometric constraints that need to be considered. Due to the chassis geometry, tubular structures depict features that trigger undesired buckling modes, e.g., Euler-type buckling. The goal of this research is to avoid such modes, particularly under oblique impact. The results need to be compared to the idealized behavior depicted by benchmark structures. Three benchmark structures are considered: (1) ideal homogeneous structure, (2) tapered geometry structure, and (3) tapered thickness structure. Critical values for oblique load angle θ were determined for uniform tube, wall angle β , and thickness angle α are determined in the following three parametric studies:

Ideal homogeneous structure:

A uniform square section tube is used. The impact plate is varied with increasing value of θ . The critical impact load angle θ_{cr} is found such that $\theta < \theta_{cr}$ leads to progressive buckling, and $\theta \geq \theta_{cr}$ leads to Euler-type buckling.

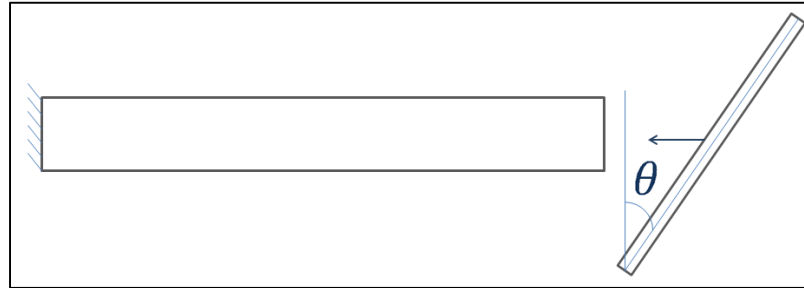


Figure 3-8: Crushing load angle θ between a rigid moving wall and the thin-walled tubular structure.

Progressive buckling was observed initially for lower angles, which can also be seen through the force displacement graph. At the critical angle $\theta_{cr} = 32^\circ$ global bending was observed which is also evident through the force displacement plots. This angle is considered to be the critical angle where the uniform tubular structure bends (Figure 3-11).

Tapered geometry structure:

This is a more deterministic design as the tapered structure would give more stability to the structure. As shown in this Figure 3-9 the wall angle β determines the tapered design. Simulations were performed for $\beta = 1^\circ$ and $\beta = 5^\circ$. The critical impact angle θ_{cr} is found out for every wall angle.

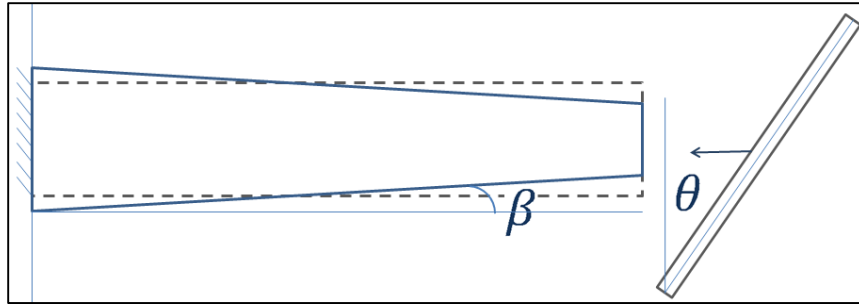


Figure 3-9: Wall angle β of a tapered structure

The tube is made tapered by a given $\beta = 1^\circ$ and $\beta = 5^\circ$ and simulations were performed by varying angle θ to obtain global bending. For $\beta = 1^\circ$ the critical angle $\theta_{cr} = 32^\circ$ global bending was observed (refer to Figure 3-12). For $\beta = 5^\circ$ the critical angle $\theta_{cr} = 64^\circ$ global bending was observed. The force displacement characteristic is studied for this idealistic structure.

Tapered thickness structure:

This is another deterministic design, which has a thickness angle α which increases the thickness from top of the tube to the bottom if the tube in a linear manner. For given thickness angle we find the critical impact angle θ_{cr} .

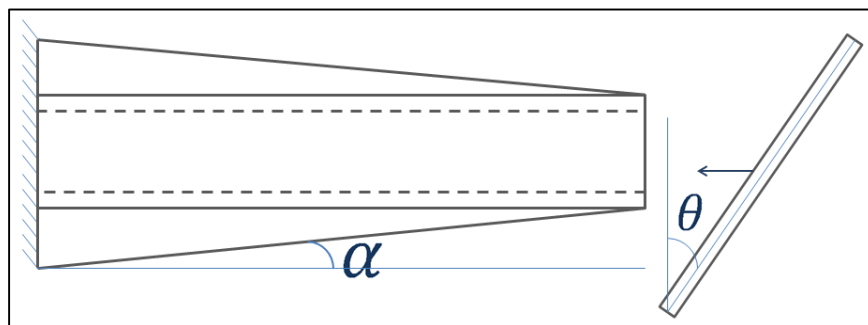


Figure 3-10: Thickness angle α of a tubular structure

For the first case $\alpha = 0.01$ the minimum and maximum thickness are 3mm and 4mm. The critical impact angle $\theta_{cr} = 59^\circ$ global bending was observed for this case. Then for the second case $\alpha = 0.01$ the minimum and maximum thickness are 3mm and 6mm. The critical impact angle $\theta_{cr} = 61^\circ$ global bending was observed.

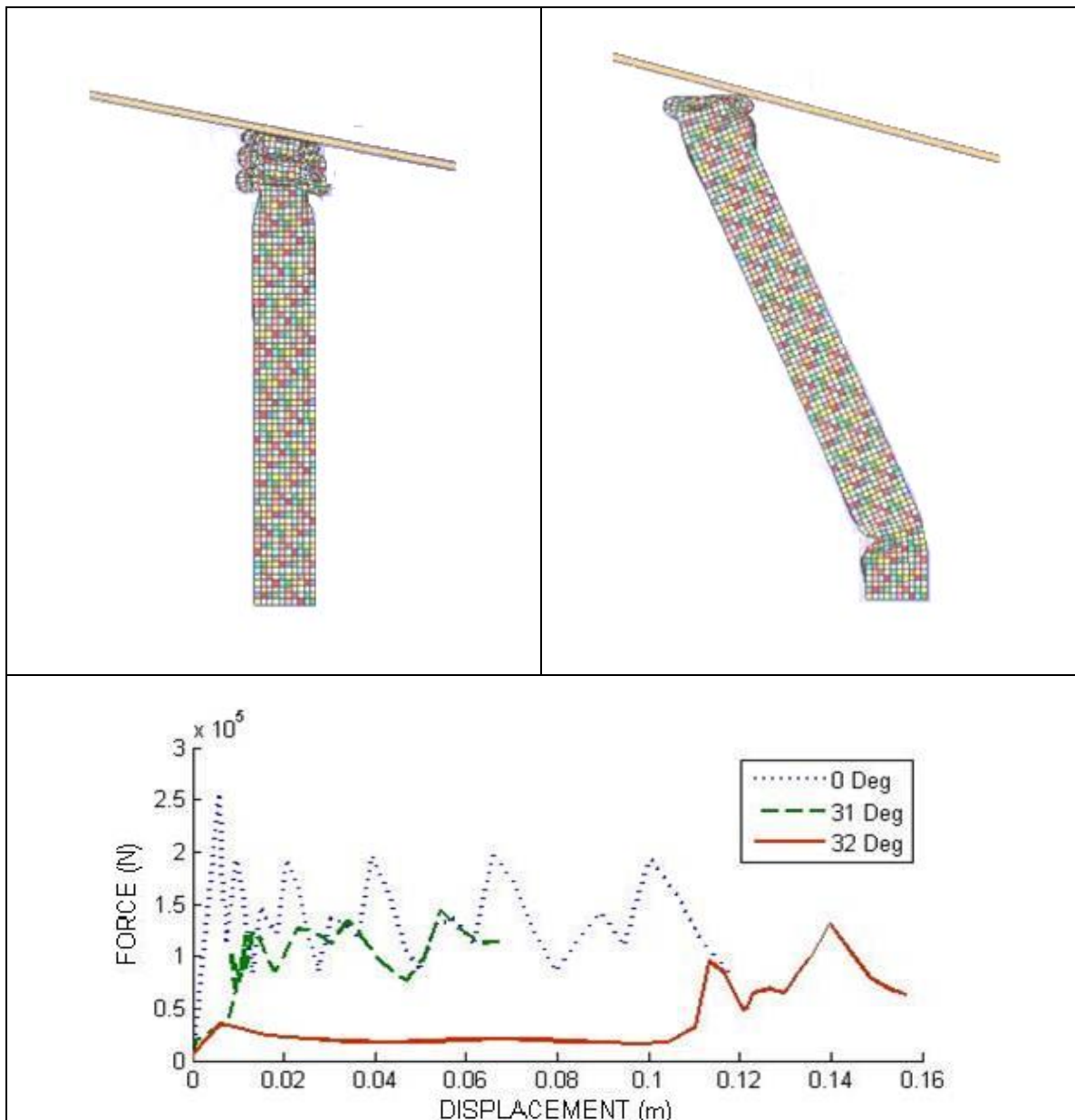


Figure 3-11: Results for critical load angle, $\theta_{cr} = 32^\circ$

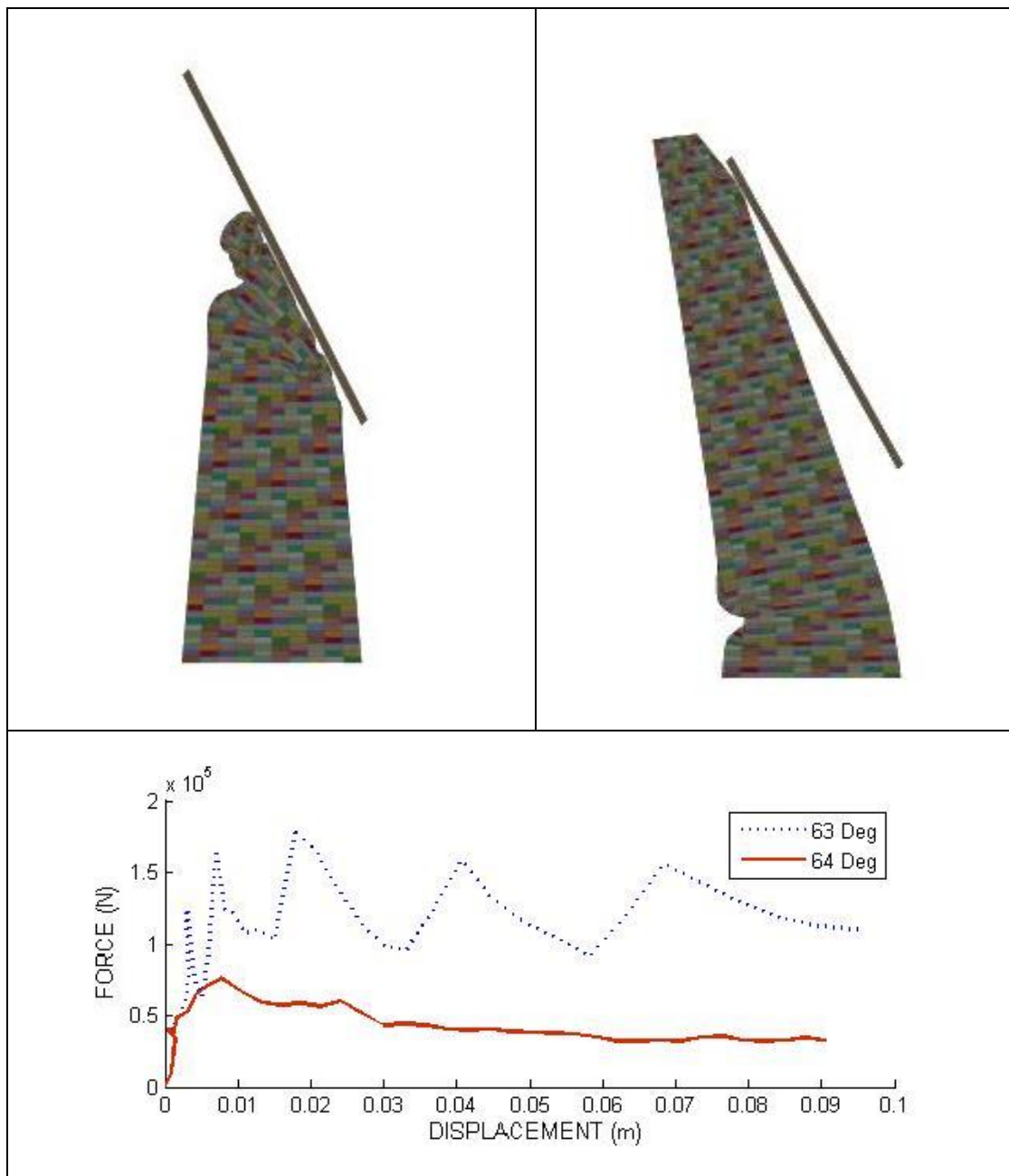


Figure 3-12: Results for critical wall angle $\beta = 5.0^\circ$ critical angle $\theta_{cr} = 64$

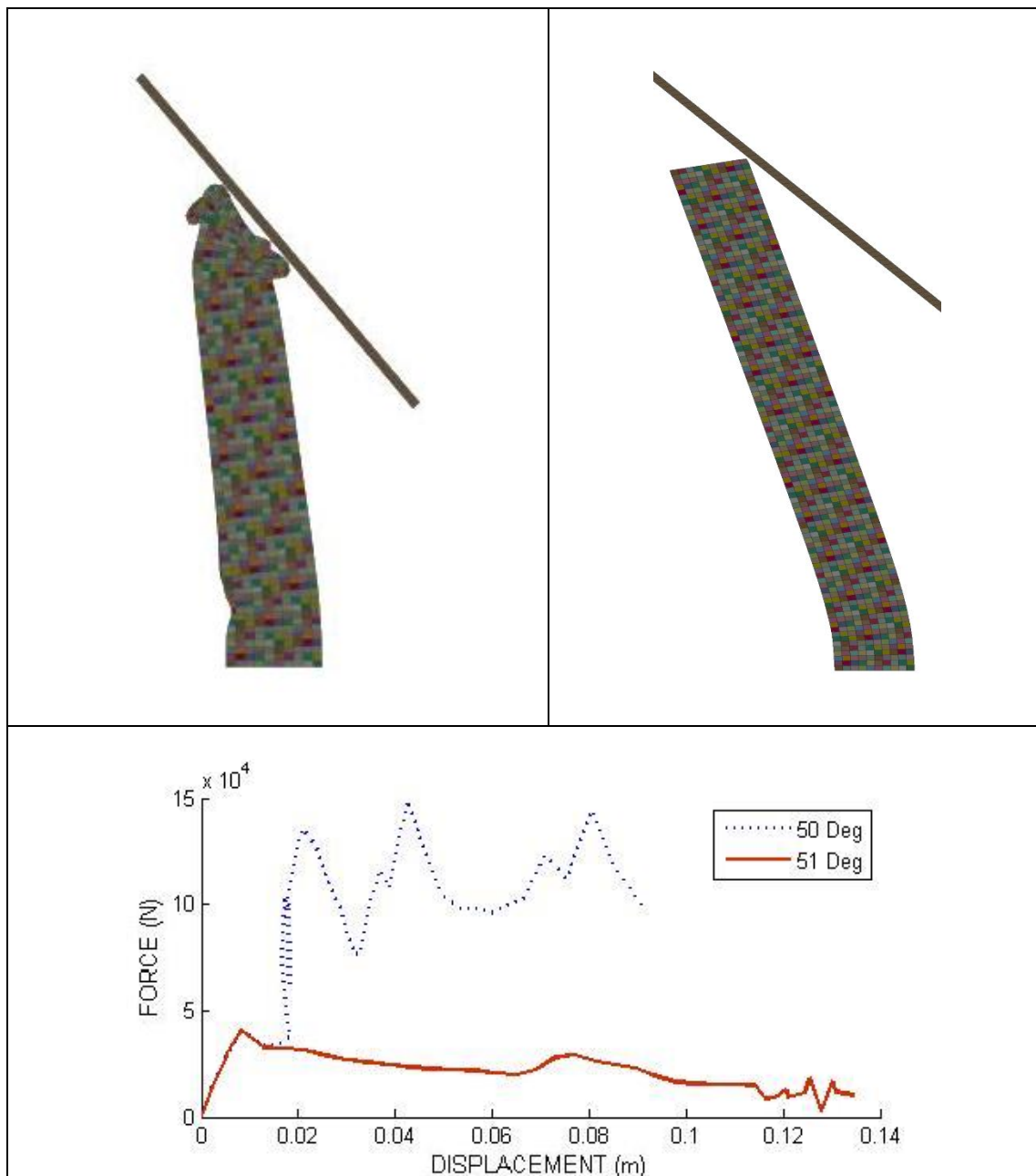


Figure 3-13: Results for critical wall angle $\alpha = 1.0^\circ$ critical angle $\theta_{cr} = 51^\circ$.

3.5.2 Geometry Definition of a Complex Tubular Structure

Geometric imperfection: We have used a tubular structure with geometric imperfection as our example. We have designed a square tube of mesh size 40x100 on each side of the tube. Each element is of size 0.01x0.01m. Each element of the tube is discretized as a different part which can also be seen though the Figure 3-14 the tube has elements with different colors. The square tube is 1m long, 0.1m in width and the thickness of the tube is 3mm. The geometric imperfection starts from 0.125m from bottom and has a length of 0.125m. The geometry is shown in the Figure 3-14. A rigid solid plate is used to crush the tube which is inclined at the θ_{cr} angle which is obtained from the benchmark procedure. The rigid plate is given a velocity of 5m/s for a prescribed displacement.

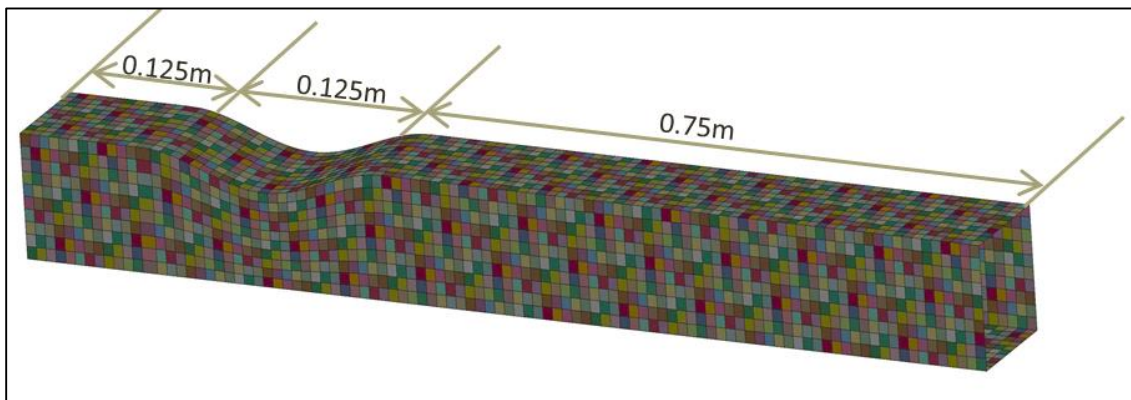


Figure 3-14 : The geometry of the tubular structure with imperfection.

S-Rail: The second example we are looking at is an S-Rail tubular structure with imperfection. The designed tube has a mesh size of 40x130 on each side. Each element is of size 0.01x0.01m. For S-rail too each element of the tube is discretized as a different part which can also be seen though the Figure 3-15 the tube has elements with different colors.

The tube is 1.13m long, 0.1m in width and thickness is of 3mm. The S-rail structure has geometry as shown in the Figure 3-15. We are using a rigid plate first with axial impact and then at a θ_{cr} angle obtained from benchmark. A velocity of 5m/s for a prescribed displacement the rigid plate is given.

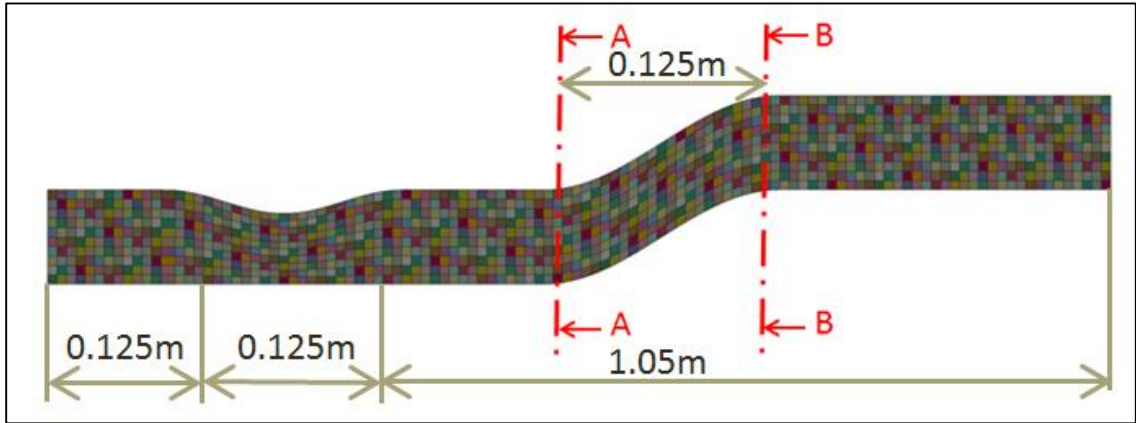


Figure 3-15 : The geometry of the tubular structure with imperfection.

3.6 Results

3.6.1 Tubular Structure with Geometric Imperfection

Tubular structures used in the real time industrial applications are usually not ideally uniform tubes. A tubular structure with imperfection is most widely used and would be an appropriate example to look at. Also one cannot assume a perfect axial impact during a real time crash event. The example we are looking at is a tubular structure with geometric imperfection and having an impact angle of 20° , θ_{cr} obtained from the benchmark. Simulations were performed on a uniform thickness tube having geometric imperfection

by crushing it with a rigid plate axially refer to Figure 3-16(a) and at an oblique impact refer to Figure 3-16(b). The buckling starts at the geometric imperfection location, which is undesirable. Euler Buckling is observed in both the designs and a high peak force is noticed.

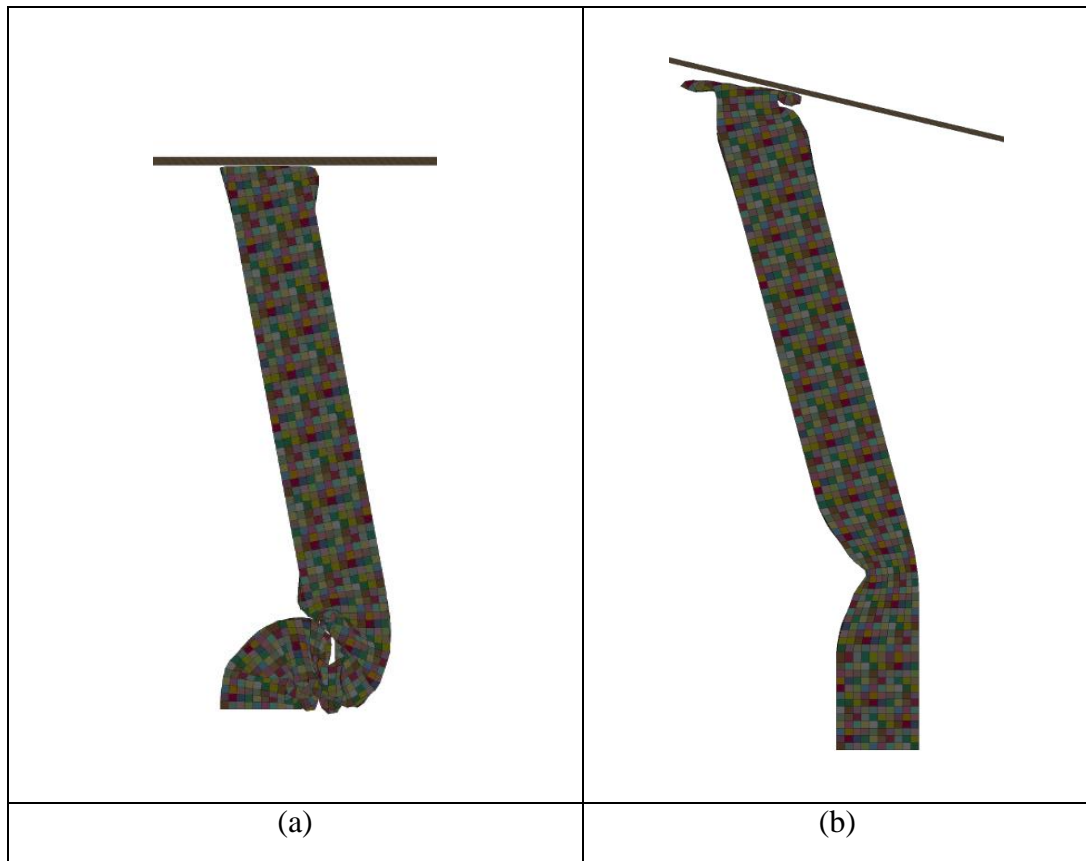


Figure 3-16: Euler buckling seen in tubular structures with imperfection.

The above uniform thickness structure is compared to the tubular structure designed through the proposed design methodology. The designed tube has the same geometry, mass and the loading conditions. The comparison for the same is shown in Table 3-2.

Table 3-2: Comparison between Uniform tube, Designs 1 and 2.

	Initial Design	Design 1	Design 2
Peak force (N)	1.3520e+5	1.1359e+5	8.9287e+4
Energy (N-m)	5.5016e+3	6.1744e+3	3.8547e+3

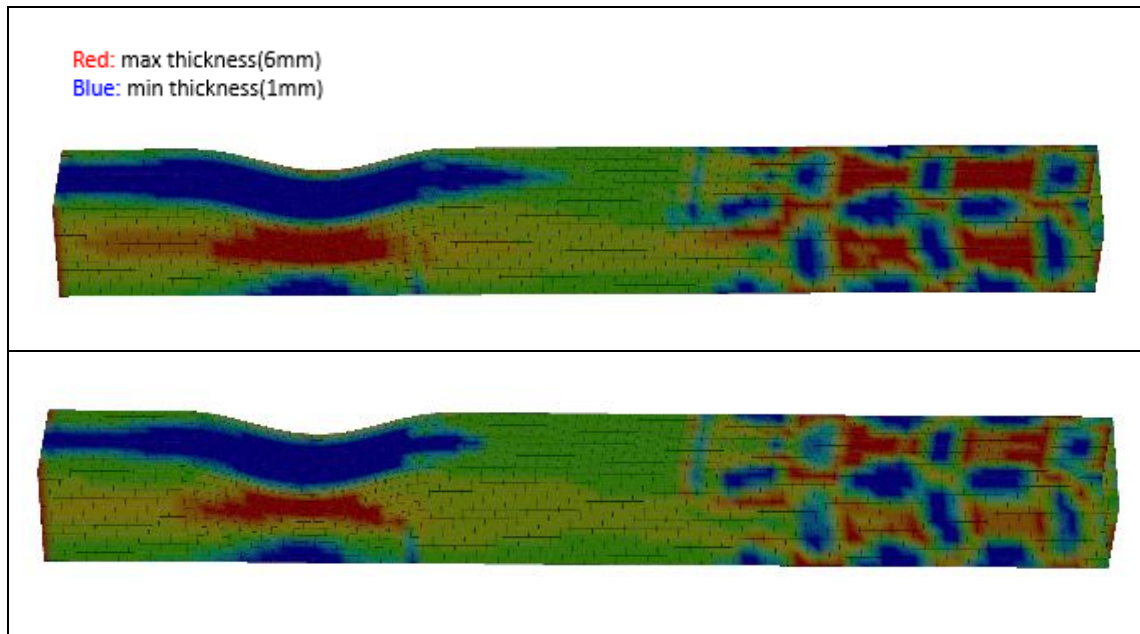


Figure 3-17: Thickness distribution for Design 1 (top) and Design 2 (bottom)

We are comparing the uniform thickness design, i.e. initial design with our 2 designs, one which is generated at iteration 56 and other at iteration 99, Figure 3-18. Most important achievement through this design methodology is to achieve progressive buckling. Euler buckling is root reason for this investigation, which now can be avoided. We can see

from the comparison that the peak force is reduced for both designs, which is a very important factor for crashworthy structure. If we further want peak force reduction we would have to compromise with the energy absorbed. The energy absorption has also increased as compared to the initial design for the same mass. The thickness distribution for the design tubes is shown in Figure 3-17.

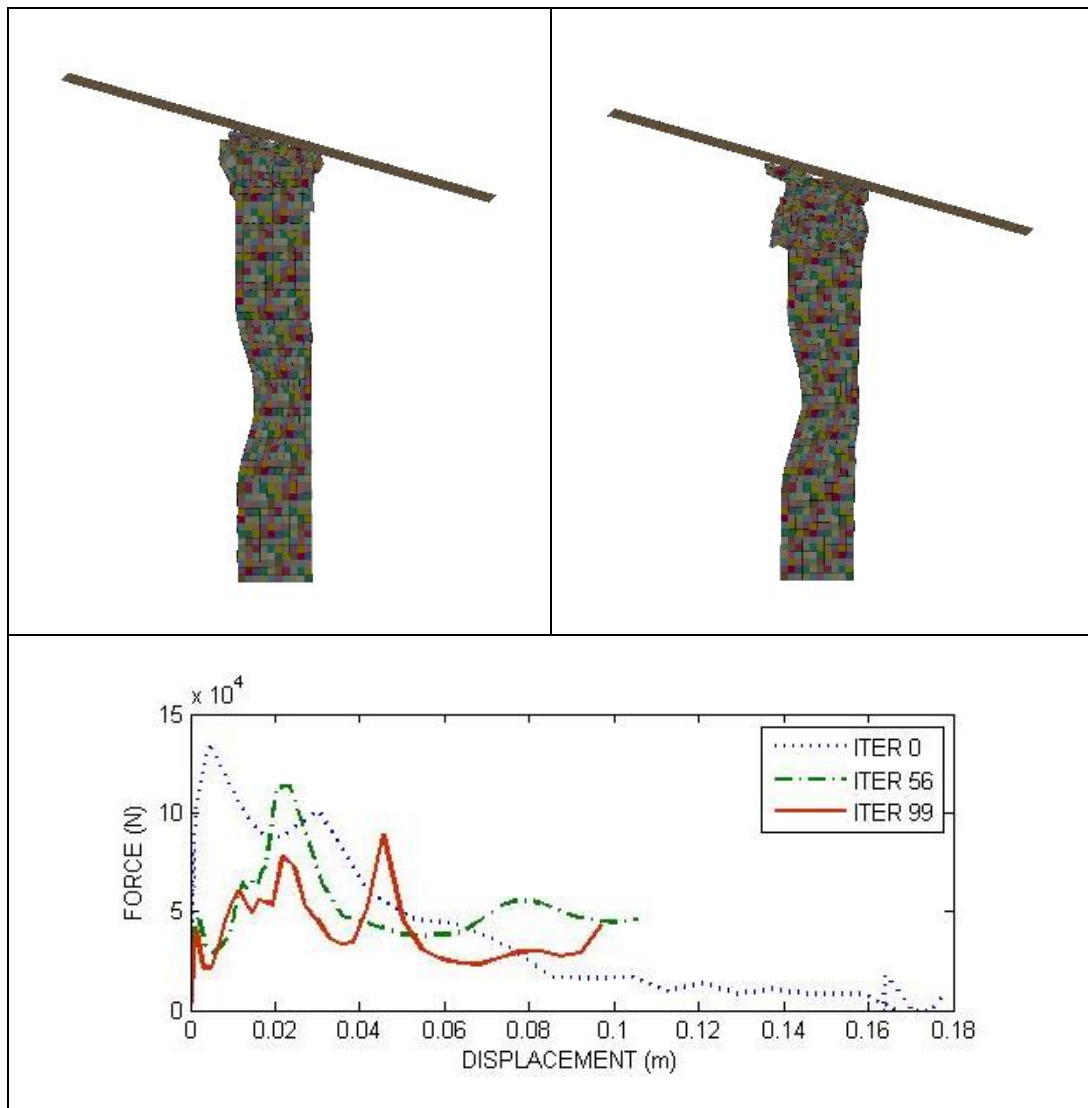


Figure 3-18: Results for the compliant tubular structure with imperfection.

3.6.2 S-Rail with Geometric Imperfection

Taking the previous example one step further, let us consider the S-Rail structure, which has added geometric complexities compared to the previous structure. These complexities would increase the number of probable locations where Euler buckling will take place. As the S-Rail structure is the most common tubular structure used in a vehicle, it is more pertinent to our study.

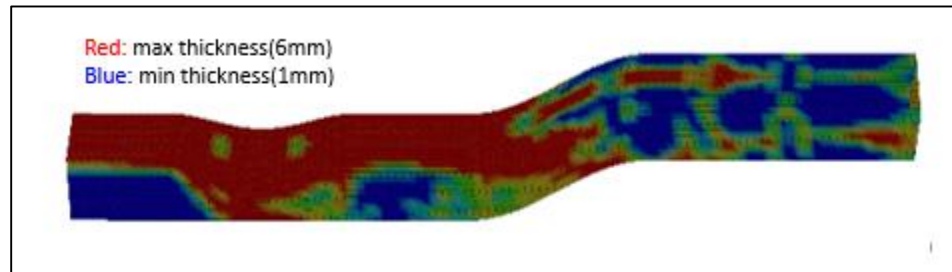


Figure 3-19 : Thickness distribution for designed tube.

In the present example the impact on the S-Rail tubular structure with imperfection is axial and at an oblique angle θ_{cr} . Initially we performed the simulation with a uniform thickness of 3mm at both axial and oblique impact. It was observed that the tube bends at the two sections A and B shown in Figure 3-15. During a real crash scenario this would cause penetration into the vehicle's 'cabin space', defined as starting at the location of Section B from the impact location. After optimizing the S-Rail through our design methodology we have achieved progressive buckling in the front "crush zone" during both types of impact. The thickness distribution for the same is shown in the Figure 3-19. Side by side comparison can be seen in Figure 3-20 for axial impact and Figure 3-21 for oblique impact. The simulation results show the behavior of S-Rail with uniform thickness and designed S-Rail at the same time steps to have a direct comparison of the modes of

deformation. The force versus displacement behavior of the final design (ITER 65) has been changed, from an early peak force followed by an immediate drop off for the initial structure, to a lower initial force building to a peak after approximately 0.1 m of stroke. We can see from the force displacement graph that there is a high peak force for the final design (ITER 65) which is due to start of penetration at section B. The initial structure, as we can see from the figures (Figure 3-20 and Figure 3-21), has global bending starting at two locations which is not at all desired.

The designed structure shows progressive buckling until it reaches section B which in comparison to uniform tube bends at both curves from the start. The designed S-Rail has a more desirable behavior with the force versus displacement growing in a progressive manner. This clearly shows the designed S-Rail structure is more efficient for the desired crashworthy performance.

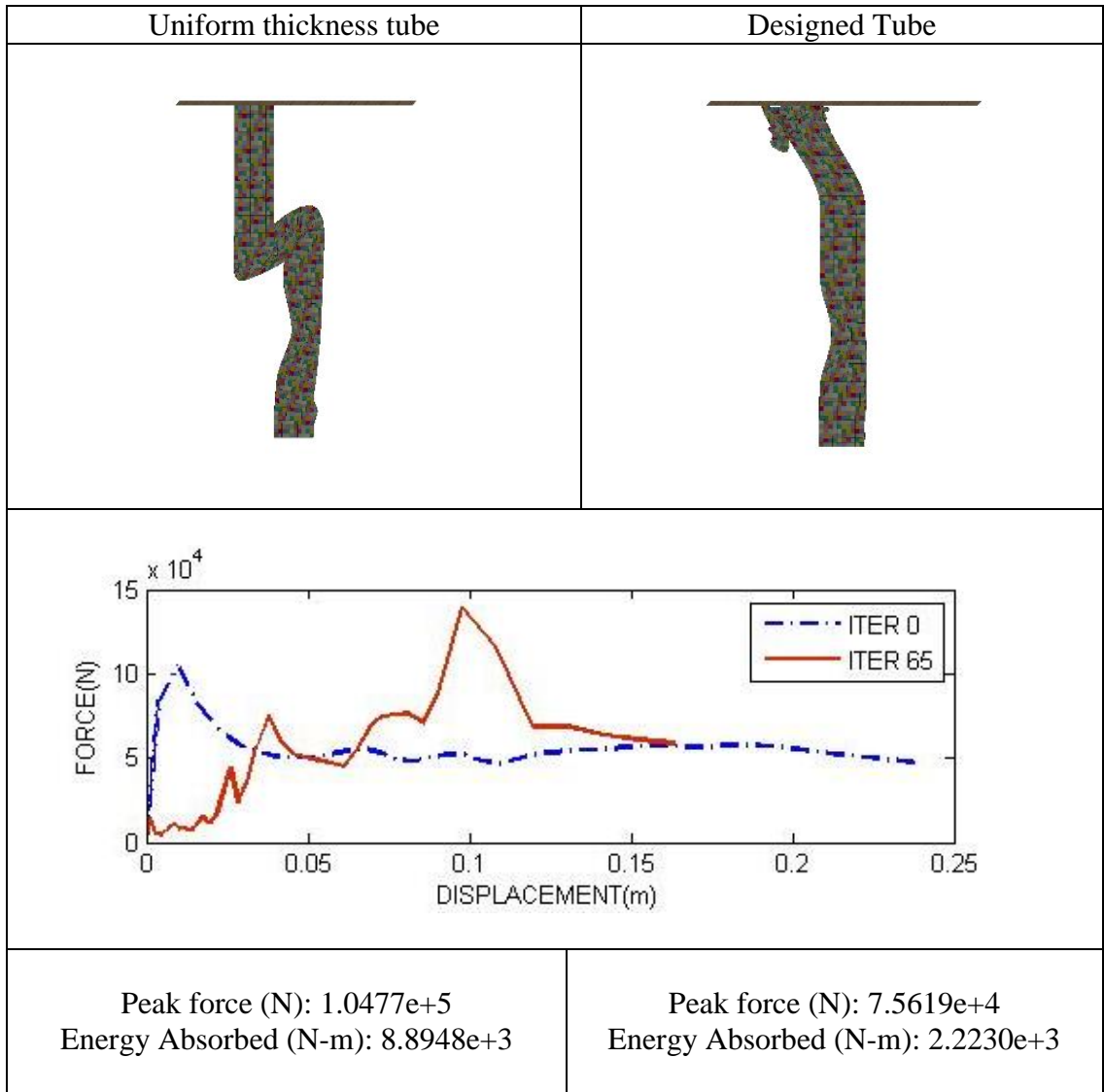


Figure 3-20: Comparison between designs for axial impact case.

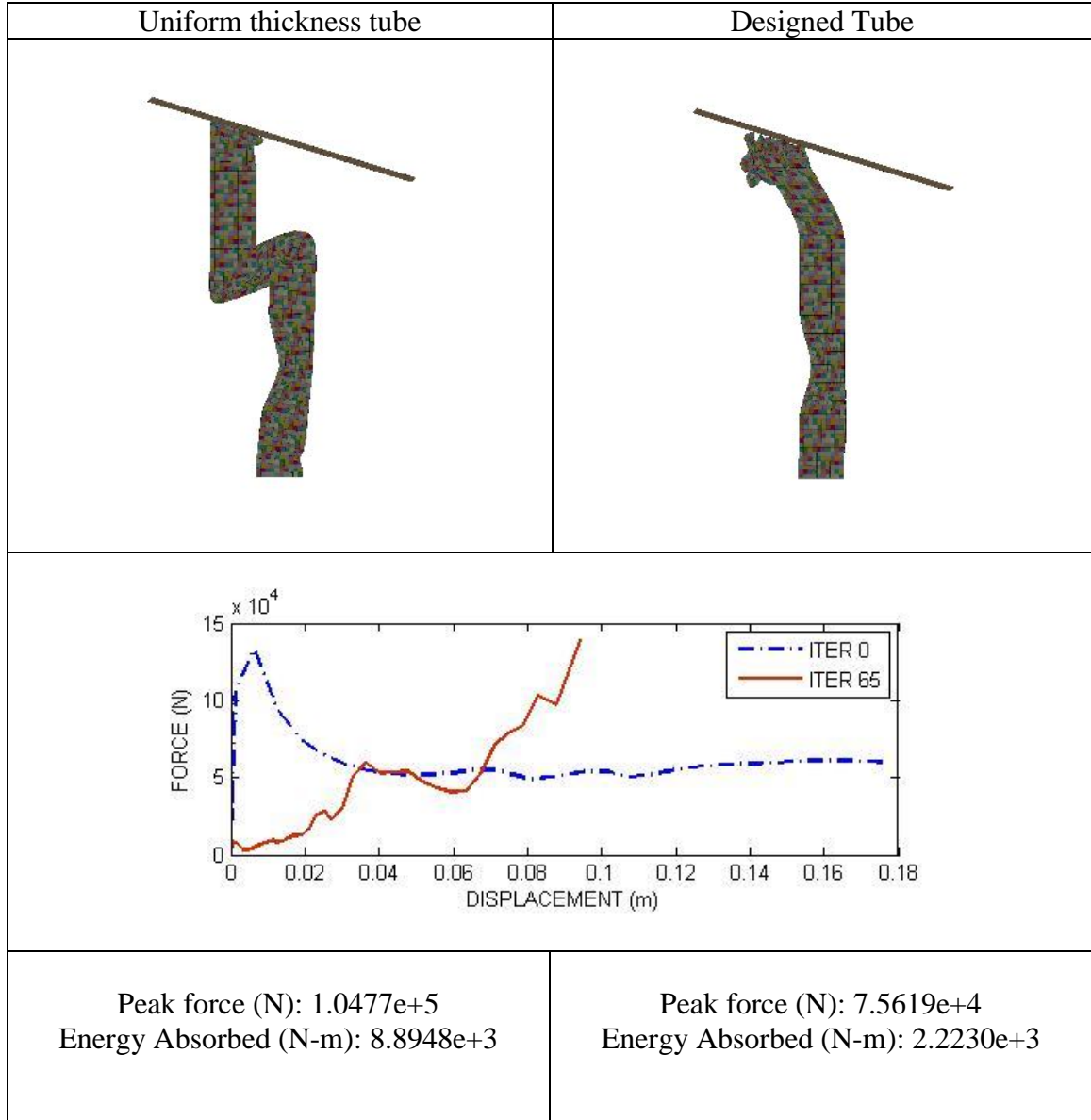


Figure 3-21: Comparison between designs for oblique impact case.

3.7 Summary of Contributions

A new method for designing thin-walled tubular structures under axial and oblique impacts based on the use of compliant mechanism synthesis is presented. Using this novel

method, square cross-sectioned tubular structures can be designed to exhibit buckling starting from the loading (impact) end and systematically progressing toward the rear end even in the presence of significant but reasonable geometric imperfections and asymmetries in the loading conditions. Three benchmark problems were evaluated to benchmark the behavior of more intuitive designs when subjected to impact. Experiments were performed to obtain critical impact angle in a conventional structure, tapered wall structure and a structure with tapered thickness along the wall. Experiments were performed using this design methodology on tubular structures with geometric imperfection and S-rail which is used in automotive design. The designed tubes through this methodology showed good progressive buckling imitating from the loading point to the fixed end. A good deformation characteristic was achieved through this design methodology. Comparing the crashworthiness indicators namely peak force and energy absorbed the design seemed to show better characteristics than a uniform thickness design.

CHAPTER 4. PROPOSED WEIGHTED APPROACH FOR THIN-WALLED TUBULAR COMPONENT SYNTHESIS

Design of thin walled tubular structures with a compliant mechanism approach has been observed to be very much effective from the previous chapters. However there is always a need of improving the stiffness of the structure. By the compliant mechanism approach we design the tube to initiate its buckling at the output port location and we achieve that by making the structure compliant or flexible. However an S-rail which connects the bumper would still need to be stiff enough to sustain low impact crash events. There are additional crash pads in the system so as to resist the lower impact. This approach is developed to give us a better control over the stiffness requirements of a structure. Here we are considering a weighted multi-objective optimization problem with minimum compliance, to increase the stiffness and compliant mechanism to achieve a good deformation characteristic.

4.1 Technical Background

A classic topology optimization problem would be to increase the stiffness of the structure for a given loading condition and mass constraint. This problem is formulated as a minimum compliance problem, where we minimize the compliance (flexibility) of the structure by adding stiffness to it. For a given vector of load f , the output displacement vector u is obtained from the structural equilibrium condition. The compliance is defined

as the scalar product of the structure's finite-element force and displacement vectors, \mathbf{F} and \mathbf{U} . The optimization problem thus can be formulated as:

$$\begin{aligned}
 \text{find :} & \quad t_i \\
 \text{minimize :} & \quad \text{Compliance} = \mathbf{f}^T \mathbf{u} \\
 \text{subject to :} & \quad r = 0 \\
 & \quad \sum_{i=1}^N t_i A_e \rho = M \\
 & \quad t_{min} \leq t_i \leq t_{max}
 \end{aligned} \tag{4.1}$$

where t_i is the design variable (thickness), A_e is the area of every element which is usually constant, ρ is the density, M is the mass and r is the residual of the structural equilibrium condition. Compliance of a structure can also be represented as:

$$\mathbf{f}^T \mathbf{u} = \sum_{i=1}^N \frac{\sigma_i \epsilon_i}{2} = \sum_{i=1}^N \frac{(SE)_i}{2} \tag{4.2}$$

where σ_i and ϵ_i are the elemental stress and strain values. $(SE)_i$ is the strain energy corresponding to every element, i.e. where $i = 1, 2, 3 \dots N$. Using the above equation in the optimization problem definition.

$$\begin{aligned}
&\text{find :} && t_i \\
&\text{minimize :} && \frac{\sigma_i \epsilon_i}{2} \\
&\text{subject to :} && r = 0 \\
&&& \sum_{i=1}^N t_i A_e \rho = M \\
&&& t_{min} \leq t_i \leq t_{max}
\end{aligned} \tag{4.3}$$

4.2 Proposed Design Methodology: Weighted Multi-Objective Approach

Tubular structures for crashworthiness application needs to be stiff to withstand the low impact events and buckle in a progressive manner when subjected to a high intensity impact. We are using a weighted approach between minimizing compliance and maximizing the mutual potential energy. The weight w is now used to have an appropriate balance between the 2 objectives, namely to minimize compliance and maximize Mutual Potential Energy.

For this problem formulation there are 3 different load cases. Figure 4-1(a) is the load case used to calculate the Strain energy so as to obtain $(SE)_i$. σ_i and ϵ_i are the stress and strains obtained from this load case which is used to compute the SE(Strain Energy) or compliance. Figure 4-1 (b) is model with loads at the input port location and springs at the output port location. Figure 4-1 (c) is the dummy load having force at the output port locations. Figure 4-1(b) and Figure 4-1 (c) are the load cases used to obtain $(MPE)_i$. The values of the stress σ_d is the stress calculated from the dummy load case Figure 4-1 (c) and the strain ϵ_{1i} from the input port load case Figure 4-1 (b). If the weight $w = 0$ the

objective function turns into a minimum compliance problem and with it turns into a compliant mechanism problem.

Following are the load cases:



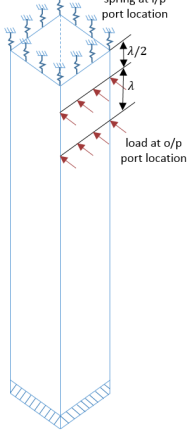
Load case 1: Normal Load	Load case 2: Input load model	Load case 3: Dummy load model
		
(a)	(b)	(c)

Figure 4-1: Load case's for tubular weighted multi-objective approach.

The Lagrangian from the optimization problem defined before.

$$\mathcal{L} = -w \left(\sum_{i=1}^n \sigma_{d_i}^T \epsilon_{1_i} \right) + (1-w) \left(\sum_{i=1}^n \frac{\sigma_i \epsilon_i}{2} \right) + \sum_{i=1}^n \lambda_{1i} (t_i - ub + s_{1i}^2) + \sum_{i=1}^n \lambda_{2i} (lb - t_i + s_{0i}^2) + \sum_{i=1}^n \lambda_v (t_i A_e \rho - M + s_v^2) \quad 4.4$$

where λ_{1i} , λ_{2i} and λ_v are the Lagrange multipliers while s_{1i} , s_{0i} and s_v are the slack variables. The necessary conditions then can be obtained as:

$$\frac{d\mathcal{L}}{dt_i} = 0 \quad \text{for } i = 1, 2, \dots, N \quad 4.5$$

$$\frac{d\mathcal{L}}{d\lambda_{1i}} = 0 \quad \text{for } i = 1, 2, \dots, N \quad 4.6$$

$$\frac{d\mathcal{L}}{d\lambda_{0i}} = 0 \quad \text{for } i = 1, 2, \dots, N \quad 4.7$$

$$\frac{d\mathcal{L}}{d\lambda_v} = 0 \quad 4.8$$

Differentiating with respect to slack variables will give switching conditions (which tells if inequality constraints are active or not) as

$$\frac{d\mathcal{L}}{ds_{1i}} = 2\lambda_{1i}s_{1i} = 0 \quad 4.9$$

$$\frac{d\mathcal{L}}{ds_{0i}} = 2\lambda_{0i}s_{0i} = 0 \quad 4.10$$

$$\frac{d\mathcal{L}}{ds_v} = 2\lambda_v s_v = 0 \quad 4.11$$

Solving the above equations we get:

$$-\frac{w(\sum_{i=1}^n(MPE)_i)}{t_i A_e \rho} + \frac{(1-w)(\sum_{i=1}^n(SE)_i)}{t_i A_e \rho} = -\frac{w(MPE)_g + (1-w)(SE)_g}{M} \quad 4.12$$

where $(MPE)_i = \boldsymbol{\sigma}_{d_i}^T \boldsymbol{\epsilon}_{1_i}$, $(SE)_i = \frac{\sigma_i \epsilon_i}{2}$, $(MPE)_g$ and $(SE)_g$ are the global mutual potential energy and strain energy. The field variable and the target values are defined from the above equation as:

$$\text{Field variable} = S_i = -\frac{w(\sum_{i=1}^n(MPE)_i)}{t_i A_e \rho} + \frac{(1-w)(\sum_{i=1}^n(SE)_i)}{t_i A_e \rho} \quad 4.13$$

$$\text{Target value} = S^* = -\frac{w(MPE)_g + (1-w)(SE)_g}{M} \quad 4.14$$

From the above field variable and target value, the optimization problem can be stated as:

$$\begin{aligned}
 \text{find :} & \quad t_i \\
 \text{minimize :} & \quad |S_i - S^*| \\
 \text{subject to :} & \quad r = 0 \\
 & \quad \sum_{i=1}^N t_i A_e \rho = M \\
 & \quad t_{min} \leq t_i \leq t_{max}
 \end{aligned} \tag{4.15}$$

To obtain an optimal design, the material is redistributed throughout the design domain in order to get uniform distribution of field variables. Accordingly, a setpoint or target is uniformly applied to all CAs in the design domain. HCA attempts to drive the state of each CA to this value. Compared to the linear static cases, gradient information can be stated as uniform field variable distribution rule in HCA. The idea of uniform distribution of field variables to get efficient designs (not necessarily optimal) comes from fully stressed design (FSD) method where the material is redistributed over the design such that all the elements contribute to the common goal efficiently.

4.3 Numerical Results

The weight w plays a very important role in this design methodology. As described earlier, the weight $w = 0$ would make the structure to be of a stiff design. This would change the problem to a single optimization problem, i.e. to minimize compliance. In the Figure 4-2 we can see a designed tube with weight $w = 0$, the tube fails due to global bending at the imperfection. Then with the weight $w = 1$ the problem is transformed to only maximize

the mutual potential energy, which is similar to the design discussed in earlier chapter. This makes the structure compliant and the tube as shown in the Figure 4-3 buckles in a progressive manner.

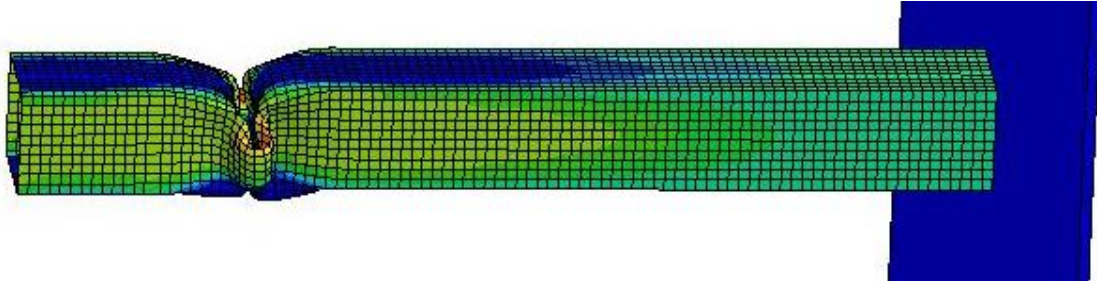


Figure 4-2: Tube with weight $w = 0$

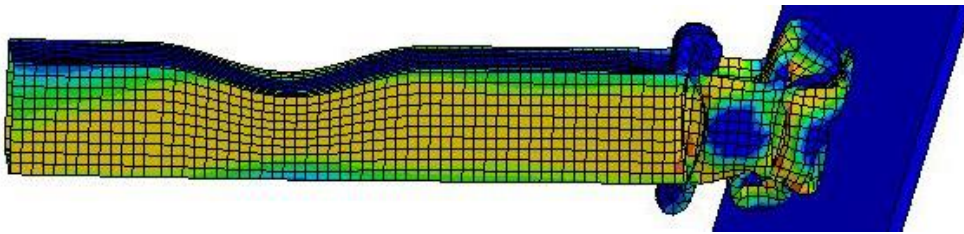


Figure 4-3: Tube with weight $w = 1$

From the above study we see the impact that the weight w has on the design at its extreme values 0 and 1. We further performed a study to see the impact of weight w with its intermediate values. A tubular structure with geometric imperfection was subjected to an oblique impact with an oblique angle α as shown in the Figure 4-4. For every design we find the maximum value of the angle of an oblique impact a structure can sustain without bending. So we choose the angle α as the measure of performance.



Figure 4-4: Tube with geometric imperfection subjected to an impact at angle α .

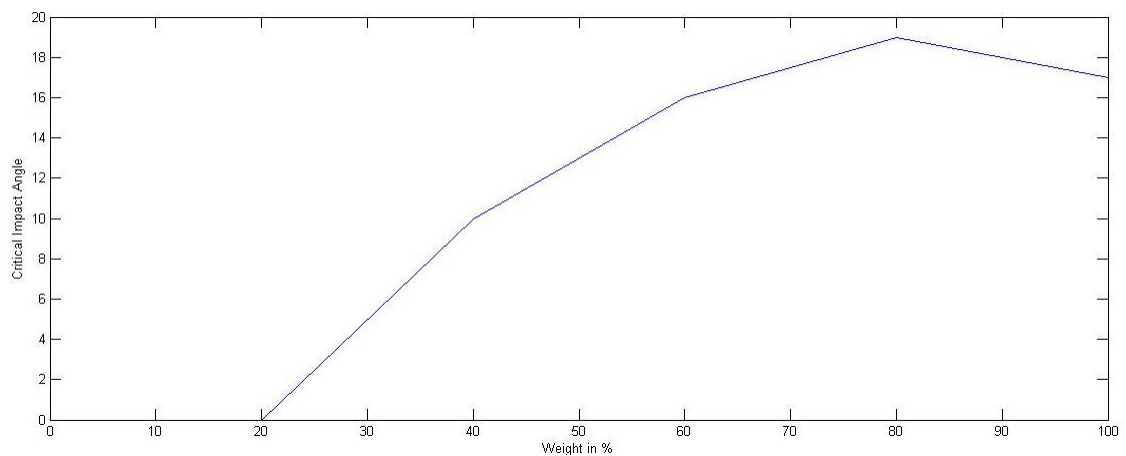


Figure 4-5: Plot of the weight (w) vs Oblique impact angle α .

From the Figure 4-5 we can see that the performance parameter α increases with increase in weight and then it would again decrease later on. This shows the addition of the Strain energy into the objective function surely increases the design performance. Below are the simulations for uniform tubular structure with geometric imperfection performed and compared with the design obtained from this methodology. The tubular structure's was subjected to axial and oblique impact. Peak force and energy absorbed are the compared.

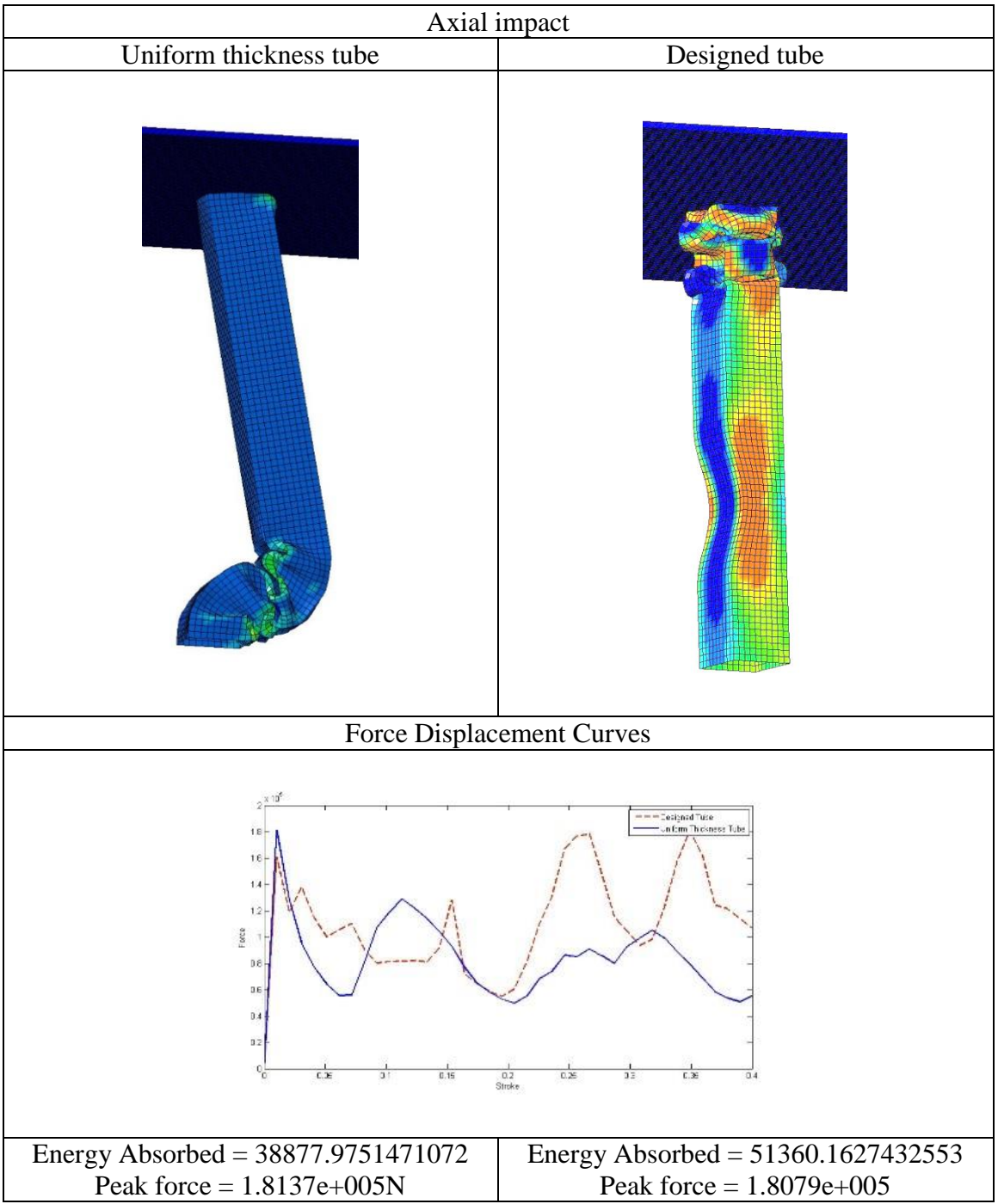


Figure 4-6: Comparison between uniform thickness tube and designed tube subjected to the axial impact

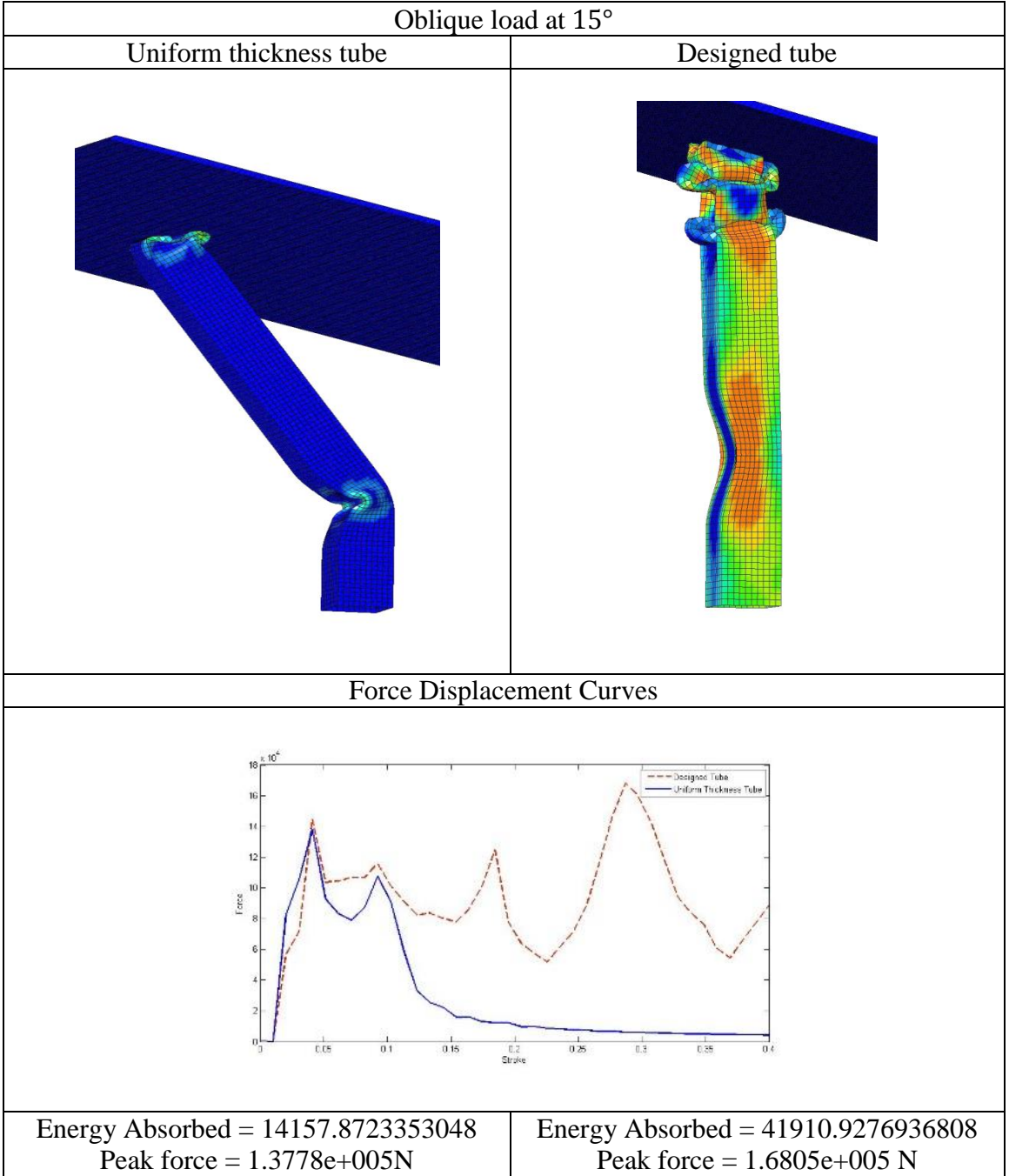


Figure 4-7: Comparison between uniform thickness tube and designed tube subjected to oblique impact.

We can clearly see from the above example that the designed tube outperforms the tube with uniform thickness in terms of deformation characteristics. We can see in case of

tube with uniform thickness, during both axial and oblique impact the tube starts to bend at the imperfection which is not desired. The designed tube has overall energy absorbed better as compared to the uniform thickness tube. However we have seen such results in the previous section while we used a compliant mechanism approach only. Following is a comparison of a designed tube from a compliant mechanism structure and a weighted multi-objective approach.

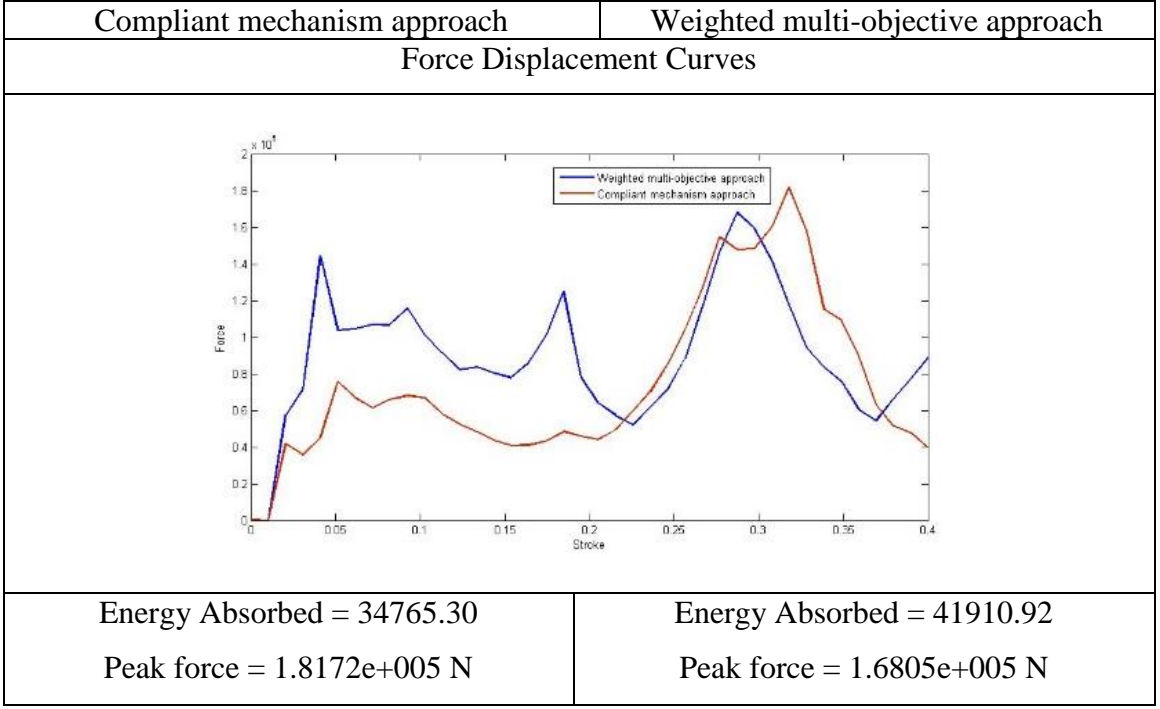


Figure 4-8: Comparison between compliant mechanism approach and weighted multi-objective approach.

From the Figure 4-8 we can see that the overall energy absorption is increased from our design through weighted multi-objective approach. Progressive buckling and a good deformation characteristic is seen in both cases. Also the initial peak force at which the buckling initiates has increased. This shows that the structure will sustain an higher impact

force compared to the previous design. If we have $w = 1$ in the weighted multi-objective approach the problem changes to the compliant mechanism approach. However by introducing a second objective function we have been successful in making the structure stiffer and still have a progressive buckling. If we want the buckling to start at a lower impact then we can use $w = 1$ or else decrease the value of w to initiate buckling at higher impact. As we increase the weight w we are increasing the stiffness and hence buckling would start at a higher impacts. There is an upper and a lower bound for this approach. For the give mass constraint and tube geometry, at $w = 1$ gives us the minimum value for impact at which the buckling can initiate. Similarly as we decrease w after a certain value the tube will more stiff than compliant and after a certain value we would not see progressive buckling.

4.4 Summary of Contributions

In this chapter we introduced the weighted multi-objective approach to design the tubular structure for crashworthiness to achieve progressive buckling. The optimization objective is redefined with a combination to maximize mutual potential energy and minimize compliance, this was achieved by using a weighting factor w . Experiments were performed to study the effect of the change in the weight w on the performance parameter α , which is the oblique impact angle. The results show an optimum design is an intermediate weight w value. Further in this chapter we compared the design from the weighted multi-objective optimization algorithm with a simple compliant mechanism design. This design approach increases the initial peak load at which the buckling initiates and increases the energy absorption compared to the previous design.

CHAPTER 5. SUMMARY AND RECOMMENDATIONS

This chapter presents an overview and general conclusions related to the work developed in this dissertation and recommendations for future work.

5.1 Summary

5.1.1 Numerical Implementation of Structural Synthesis for Crashworthiness Using

HCA

1. Successful incorporation of the HCA synthesis was demonstrated.
2. Analysis of high-fidelity crash simulations which requires hours to execute, makes gradient-based optimization techniques impractical in terms of computational time and effort. The gradient free HCA based topometry optimization algorithm used in this work demonstrates efficiency in that only one finite element analysis (FEA) is required per synthesis iteration.
3. Example 1: Topology synthesis of a bumper-like structure was performed using HCA. Improved energy absorption with reduced mass was achieved.
4. Example 2: Topography synthesis was performed on the base plate to reduce its penetration. Results showed a better penetration compared to the initial structure.

5.1.2 Structural Synthesis of Thin-Walled Tubular Components

1. Design methodology using a compliant mechanism approach was developed to design thin-walled crashworthy structures with geometric imperfections and subjected to oblique impact.
2. Numerical experiments were performed on square cross-sectioned tubular structures with geometric imperfections and S-rail structures.
3. Progressive buckling with a good deformation characteristic was achieved through this design methodology. The designed tube exhibit buckling starting from the loading (impact) end and systematically progressing toward the rear end even in the presence of significant but reasonable geometric imperfections and asymmetries in the loading conditions.

5.1.3 Proposed Weighted Approach for Thin-Walled Tubular Component Synthesis

1. Extending the above design methodology further a weighted approach was introduced. The optimization objective is redefined with a combination to maximize mutual potential energy and minimize compliance, this was achieved by using a weighting factor w .
2. Experiments were performed to study the effect of the change in the weight w on the performance parameter α , which is the oblique impact angle. The results show an optimum design is an intermediate weight w value.
3. Further in this chapter we compared the design from the weighted multi-objective optimization algorithm with a simple compliant mechanism design. This design

approach increases the initial peak load at which the buckling initiates and increases the energy absorption compared to the previous design.

4. The results of this research depict concept designs for tubular structures with variable local thickness throughout; however, the manufacturing challenges of such concept designs need to be addressed. One possible approach to address this is additive manufacturing methods.

5.2 Original Contributions

In this research we have incorporated the compliant mechanism approach to establish the design methodology for the design of thin walled tubular structures with geometric imperfection subjected to axial and oblique impact. This design methodology was then used to design the automotive S-rail which has more complex geometry. In this research we have introduced a weighted objective approach between a compliant mechanism design formulation and a minimum compliance problem. This approach helped improve the design further to have better control on the initial peak force and to sustain oblique impact at higher impact angles.

5.3 Future Recommendations

1. This proposed design methodology may be utilized in tubular structure design with variable local mechanical properties of hardness and strength. Such variable mechanical properties may be achieved by localized thermal treatments for conventionally manufactured metallic structures.

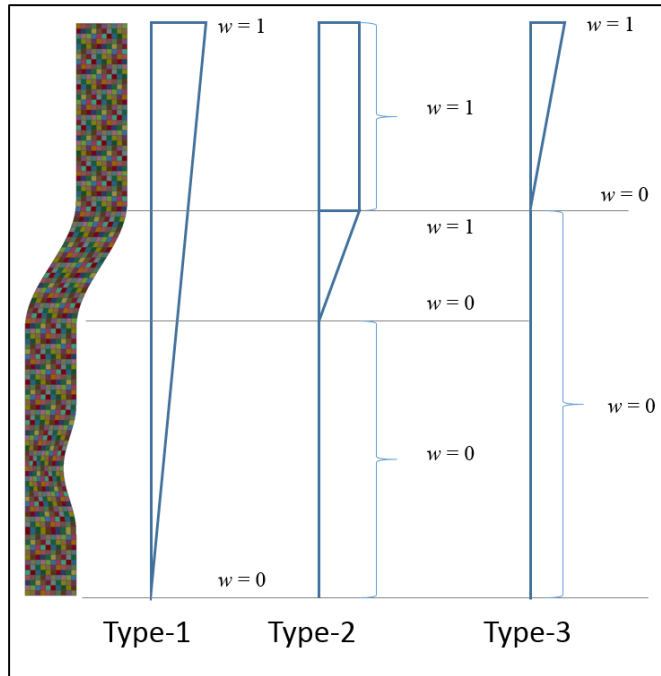


Figure 5-1: Recommendation to extend the weighted multi-objective approach.

2. The multi-objective weighted approach can be extended to vary the weight over the structure. Figure 5-1 shows three types of approaches which can be used. The Lower part of the structure needs to be stiffer compared to the upper portion to achieve a progressive buckling starting from top to bottom.
3. A combined approach using foam filled tubes and buckling initiators needs to be studied. Experiments could be performed with foam filled structures and tubes designed via a compliant mechanism approach.
4. With the requirements for crashworthiness these tubes also need to satisfy the NVH, durability and other attribute requirements. A multi-disciplinary approach should be considered to have a more robust design.

LIST OF REFERENCES

LIST OF REFERENCES

- [1] N.H.T S. Administration., "Motor vehicle crashes: overview. Report no. DOT HS-811-856. Washington, DC: US Department of Transportation.," 2012.
- [2] IIHS. (2012). *General statistics for fatality facts*. Available: <http://www.iihs.org/iihs/topics/t/general-statistics/fatalityfacts/overview-of-fatality-facts>
- [3] I. News, "Declining death rates due to safer vehicles, not better drivers or improved roadways," 2006.
- [4] M. P. Bendsoe, *Topology optimization: theory, methods and applications*: Springer, 2003.
- [5] A. Pugsley, "The large-scale crumpling of thin cylindrical columns," *The Quarterly Journal of Mechanics and Applied Mathematics*, vol. 13, pp. 1-9, 1960.
- [6] J. M. Alexander, "An approximate analysis of the collapse of thin cylindrical shells under axial loading," *The Quarterly Journal of Mechanics and Applied Mathematics*, vol. 13, pp. 10-15, 1960.
- [7] W. Abramowicz and N. Jones, "Dynamic progressive buckling of circular and square tubes," *International Journal of Impact Engineering*, vol. 4, pp. 243-270, 1986.
- [8] W. Abramowicz and N. Jones, "Dynamic axial crushing of circular tubes," *International Journal of Impact Engineering*, vol. 2, pp. 263-281, 1984.
- [9] W. Abramowicz and N. Jones, "Dynamic axial crushing of square tubes," *International Journal of Impact Engineering*, vol. 2, pp. 179-208, 1984.
- [10] W. Abramowicz, "The effective crushing distance in axially compressed thin-walled metal columns," *International Journal of Impact Engineering*, vol. 1, pp. 309-317, 1983.
- [11] T. Wierzbicki and W. Abramowicz, "On the Crushing Mechanics of Thin-Walled Structures," *Journal of Applied Mechanics*, vol. 50, pp. 727-734, 1983.

- [12] N. Jones, *Structural Impact*: Cambridge University Press, 1997.
- [13] Ø. Jensen, M. Langseth, and O. Hopperstad, "Experimental investigations on the behaviour of short to long square aluminium tubes subjected to axial loading," *International Journal of Impact Engineering*, vol. 30, pp. 973-1003, 2004.
- [14] N. Jones, *Structural impact*: Cambridge University Press, 2011.
- [15] R. T. Haftka, Z. Gürdal, and M. Kamat, "Elements of structural optimization. 1992," ed: Kluwer Academic Publishers, Dordrecht.
- [16] L. A. Schmit, "Structural synthesis-its genesis and development," *AIAA Journal*, vol. 19, pp. 1249-1263, 1981.
- [17] G. I. Rozvany, *Structural design via optimality criteria*: Springer, 1989.
- [18] K. Suzuki and N. Kikuchi, "A homogenization method for shape and topology optimization," *Computer methods in applied mechanics and engineering*, vol. 93, pp. 291-318, 1991.
- [19] S. Nishiwaki, M. I. Frecker, S. Min, and N. Kikuchi, "Topology optimization of compliant mechanisms using the homogenization method," 1998.
- [20] A. Diaz and M. Bendsøe, "Shape optimization of structures for multiple loading conditions using a homogenization method," *Structural Optimization*, vol. 4, pp. 17-22, 1992.
- [21] G. Allaire, F. Jouve, and H. Maillot, "Topology optimization for minimum stress design with the homogenization method," *Structural and Multidisciplinary Optimization*, vol. 28, pp. 87-98, 2004.
- [22] G. Allaire, Z. Belhachmi, and F. Jouve, "The homogenization method for topology and shape optimization. Single and multiple loads case," *Revue européenne des éléments finis*, vol. 5, pp. 649-672, 1996.
- [23] G. Allaire, *Shape optimization by the homogenization method* vol. 146: Springer, 2002.
- [24] M. P. Bendsøe and N. Kikuchi, "Generating optimal topologies in structural design using a homogenization method," *Computer methods in applied mechanics and engineering*, vol. 71, pp. 197-224, 1988.
- [25] H. A. Eschenauer and N. Olhoff, "Topology optimization of continuum structures: A review*," *Applied Mechanics Reviews*, vol. 54, pp. 331-390, 2001.

- [26] G. Rozvany, "Aims, scope, methods, history and unified terminology of computer-aided topology optimization in structural mechanics," *Structural and Multidisciplinary Optimization*, vol. 21, pp. 90-108, 2001.
- [27] M. P. Bendsoe and O. Sigmund, *Topology optimization: theory, methods and applications*: Springer, 2003.
- [28] K. Svanberg, "The method of moving asymptotes—a new method for structural optimization," *International journal for numerical methods in engineering*, vol. 24, pp. 359-373, 1987.
- [29] U. Kirsch, *Structural optimization*: Springer, 1993.
- [30] B. Hassani and E. Hinton, "A review of homogenization and topology optimization III—topology optimization using optimality criteria," *Computers & structures*, vol. 69, pp. 739-756, 1998.
- [31] Y.-M. Xie and G. P. Steven, "Evolutionary structural optimization," 1997.
- [32] A. Tovar, "Bone Remodeling as a Hybrid Cellular Automaton Optimization Process. PhD Disertation, University of Notre Dame, 2004."
- [33] A. Tovar, N. M. Patel, G. L. Niebur, M. Sen, and J. E. Renaud, "Topology optimization using a hybrid cellular automaton method with local control rules," *Journal of Mechanical Design*, vol. 128, pp. 1205-1216, 2006.
- [34] A. Tovar, N. Patel, A. K. Kaushik, G. A. Letona, J. E. Renaud, and B. Sanders, "Hybrid cellular automata: a biologically-inspired structural optimization technique," in *10th AIAA/ISSMO Symposium on Multidisciplinary Analysis and Optimization*, 2004.
- [35] R. R. Mayer, N. Kikuchi, and R. A. Scott, "Application of topological optimization techniques to structural crashworthiness," *International Journal for Numerical Methods in Engineering*, vol. 39, pp. 1383-1403, 1996.
- [36] R. Lust, "Structural optimization with crashworthiness constraints," *Structural Optimization*, vol. 4, pp. 85-89, 1992.
- [37] C. B. Pedersen, "Topology optimization design of crushed 2D-frames for desired energy absorption history," *Structural and Multidisciplinary Optimization*, vol. 25, pp. 368-382, 2003.
- [38] C. B. Pedersen, "Crashworthiness design of transient frame structures using topology optimization," *Computer Methods in Applied Mechanics and Engineering*, vol. 193, pp. 653-678, 2004.

- [39] C. Soto, "Structural topology optimization for crashworthiness," *International journal of crashworthiness*, vol. 9, pp. 277-283, 2004.
- [40] C. A. Soto, "Structural topology optimisation: from minimising compliance to maximising energy absorption," *International Journal of Vehicle Design*, vol. 25, pp. 142-163, 2001.
- [41] J. Forsberg and L. Nilsson, "Topology optimization in crashworthiness design," *Structural and Multidisciplinary Optimization*, vol. 33, pp. 1-12, 2007.
- [42] N. M. Patel, A. Tovar, B.-S. Kang, and J. E. Renaud, "Crashworthiness design using topology optimization," *Journal of Mechanical Design*, vol. 131, p. 061013, 2009.
- [43] P. H. Thornton and C. L. Magee, "The Interplay of Geometric and Materials Variables in Energy Absorption," *Journal of Engineering Materials and Technology*, vol. 99, pp. 114-120, 1977.
- [44] N. Chase, R. C. Averill, and R. Sidhu, "Design optimization of progressively crushing rails," *SAE world congress & exhibition*, 2009.
- [45] H. El-Hage, P. K. Mallick, and N. Zamani, "A numerical study on the quasi-static axial crush characteristics of square aluminum tubes with chamfering and other triggering mechanisms," *International Journal of Crashworthiness*, vol. 10, pp. -183-196, 2005.
- [46] S. Lee, C. Hahn, M. Rhee, and J.-E. Oh, "Effect of triggering on the energy absorption capacity of axially compressed aluminum tubes," *Materials & design*, vol. 20, pp. 31-40, 1999.
- [47] I. Eren, Y. Gür, and Z. Aksoy, "Finite element analysis of collapse of front side rails with new types of crush initiators," *International Journal of Automotive Technology*, vol. 10, pp. 451-457, 2009.
- [48] L. Abah, A. Limam, and M. Dejeammes, "Effects of cutouts on static and dynamic behaviour of square aluminium extrusions," in *Fifth international conference on structures under shock and impact, Greece*, 1998, pp. 122-31.
- [49] M. Shakeri, R. Mirzaeifar, and S. Salehghaffari, "New insights into the collapsing of cylindrical thin-walled tubes under axial impact load," *Proceedings of the Institution of Mechanical Engineers, Part C: Journal of Mechanical Engineering Science*, vol. 221, pp. 869-885, 2007.

- [50] G. Daneshi and S. Hosseinipour, "Grooves effect on crashworthiness characteristics of thin-walled tubes under axial compression," *Materials & design*, vol. 23, pp. 611-617, 2002.
- [51] G. Nagel and D. Thambiratnam, "Computer simulation and energy absorption of tapered thin-walled rectangular tubes," *Thin-Walled Structures*, vol. 43, pp. 1225-1242, 2005.
- [52] G. M. Nagel and D. P. Thambiratnam, "Dynamic simulation and energy absorption of tapered thin-walled tubes under oblique impact loading," *International journal of impact engineering*, vol. 32, pp. 1595-1620, 2006.
- [53] G. Nagel and D. Thambiratnam, "A numerical study on the impact response and energy absorption of tapered thin-walled tubes," *International journal of mechanical sciences*, vol. 46, pp. 201-216, 2004.
- [54] H. Chai, "On optimizing crash energy and load-bearing capacity in cellular structures," *International Journal of Solids and Structures*, vol. 45, pp. 528-539, 2008.
- [55] H.-S. Kim, W. Chen, and T. Wierzbicki, "Weight and crash optimization of foam-filled three-dimensional "S" frame," *Computational mechanics*, vol. 28, pp. 417-424, 2002.
- [56] S. Santosa and T. Wierzbicki, "Crash behavior of box columns filled with aluminum honeycomb or foam," *Computers and Structures*, vol. 68, pp. 343-367, 1998.
- [57] A. G. Hanssen, M. Langseth, and O. S. Hopperstad, "Static and dynamic crushing of circular aluminium extrusions with aluminium foam filler," *International Journal of Impact Engineering*, vol. 24, pp. 475-507, 2000.
- [58] X. Zhang and G. Cheng, "A comparative study of energy absorption characteristics of foam-filled and multi-cell square columns," *International Journal of Impact Engineering*, vol. 34, pp. 1739-1752, 2007.
- [59] L. Mirfendereski, M. Salimi, and S. Ziaei-Rad, "Parametric study and numerical analysis of empty and foam-filled thin-walled tubes under static and dynamic loadings," *International Journal of Mechanical Sciences*, vol. 50, pp. 1042-1057, 2008.
- [60] H. Zarei and M. Kröger, "Bending behavior of empty and foam-filled beams: Structural optimization," *International Journal of Impact Engineering*, vol. 35, pp. 521-529, 2008.

- [61] H. Zarei and M. Kröger, "Optimum honeycomb filled crash absorber design," *Materials & Design*, vol. 29, pp. 193-204, 2008.
- [62] Z. Ahmad, D. Thambiratnam, and A. Tan, "Dynamic energy absorption characteristics of foam-filled conical tubes under oblique impact loading," *International Journal of Impact Engineering*, vol. 37, pp. 475-488, 2010.
- [63] S. Salehghaffari, M. Tajdari, M. Panahi, and F. Mokhtarnezhad, "Attempts to improve energy absorption characteristics of circular metal tubes subjected to axial loading," *Thin-Walled Structures*, vol. 48, pp. 379-390, 2010.
- [64] E. Acar, M. Guler, B. Gerceker, M. Cerit, and B. Bayram, "Multi-objective crashworthiness optimization of tapered thin-walled tubes with axisymmetric indentations," *Thin-Walled Structures*, vol. 49, pp. 94-105, 2011.
- [65] S. Hou, X. Han, G. Sun, S. Long, W. Li, X. Yang, *et al.*, "Multiobjective optimization for tapered circular tubes," *Thin-Walled Structures*, vol. 49, pp. 855-863, 2011.
- [66] G. Sun, G. Li, S. Hou, S. Zhou, W. Li, and Q. Li, "Crashworthiness design for functionally graded foam-filled thin-walled structures," *Materials Science and Engineering: A*, vol. 527, pp. 1911-1919, 2010.
- [67] H. Yin, G. Wen, S. Hou, and Q. Qing, "Multiobjective crashworthiness optimization of functionally lateral graded foam-filled tubes," *Materials & Design*, vol. 44, pp. 414-428, 2013.
- [68] H. Yin, G. Wen, H. Fang, Q. Qing, X. Kong, J. Xiao, *et al.*, "Multiobjective crashworthiness optimization design of functionally graded foam-filled tapered tube based on dynamic ensemble metamodel," *Materials & Design*, vol. 55, pp. 747-757, 2014.
- [69] H. Yin, G. Wen, Z. Liu, and Q. Qing, "Crashworthiness optimization design for foam-filled multi-cell thin-walled structures," *Thin-Walled Structures*, vol. 75, pp. 8-17, 2014.
- [70] A. Reyes, O. Hopperstad, and M. Langseth, "Aluminum foam-filled extrusions subjected to oblique loading: experimental and numerical study," *International journal of solids and structures*, vol. 41, pp. 1645-1675, 2004.
- [71] M. Seitzberger, F. G. Rammerstorfer, H. P. Degischer, and R. Gradinger, "Crushing of axially compressed steel tubes filled with aluminium foam," *Acta Mechanica*, vol. 125, pp. 93-105, 1997.

- [72] P. Bandi, *Design of crashworthy structures with controlled behavior in HCA framework*, 2012.
- [73] P. Bandi, C. K. Mozumder, A. Tovar, and J. E. Renaud, "Design of Axially Crushing Thin-Walled Square Tubes using Compliant Mechanism Approach," *The American Institute of Aeronautics and Astronautics* 2010.
- [74] P. Duysinx and M. P. Bendsøe, "Topology optimization of continuum structures with local stress constraints," *International Journal for Numerical Methods in Engineering*, vol. 43, pp. 1453-1478, 1998.
- [75] R. Lipton, "Design of functionally graded composite structures in the presence of stress constraints," *International journal of solids and structures*, vol. 39, pp. 2575-2586, 2002.
- [76] A. Tovar, N. M. Patel, G. L. Niebur, M. Sen, and J. E. Renaud, "Topology optimization using a hybrid cellular automaton method with local control rules," *Journal of Mechanical Design*, vol. 128, p. 1205, 2006.
- [77] H. A. Eschenauer and N. Olhoff, "Topology optimization of continuum structures: a review," *Applied Mechanics Reviews*, vol. 54, pp. 331-389, 2001.
- [78] M. P. Bendsøe, N. Olhoff, and O. Sigmund, *IUTAM Symposium on Topological Design Optimization of Structures, Machines and Materials: Status and Perspectives*: Springer, 2006.
- [79] S. Wolfram, *A new kind of science* vol. 5: Wolfram media Champaign, 2002.
- [80] P. Pedersen, "On optimal shapes in materials and structures," *Structural and multidisciplinary optimization*, vol. 19, pp. 169-182, 2000.
- [81] O. Sigmund, "On the Design of Compliant Mechanisms Using Topology Optimization*," *Journal of Structural Mechanics*, vol. 25, pp. 493-524, 1997.
- [82] D. C. Han and S. H. Park, "Collapse behavior of square thin-walled columns subjected to oblique loads," *Thin-Walled Structures*, vol. 35, pp. 167-184, 1999.
- [83] A. Reyes, M. Langseth, and O. S. Hopperstad, "Crashworthiness of aluminum extrusions subjected to oblique loading: experiments and numerical analyses," *International Journal of Mechanical Sciences*, vol. 44, pp. 1965-1984, 2002.
- [84] P. Bandi, A. Tovar, and J. E. Renaud, *Design of 2D and 3D non-linear compliant mechanisms using hybrid cellular automata*. Denver, CO, 2011.

- [85] C. A. Narváez, A. Tovar, and D. A. Garzón, "Topology synthesis of compliant mechanisms using the hybrid cellular automaton method with an efficient mass control strategy," III European Conference on Computational Mechanics Solids, Structures and Coupled Problems in Engineering (ECCM 2006), Lisbon, Portugal, 2006.
- [86] O. Sigmund, "On the Design of Compliant Mechanisms Using Topology Optimization," *Mech. Struct. & Machines*, vol. 25, pp. 495-526, 1997.
- [87] S. Nishiwaki, M. I. Frecker, S. Min, and N. Kikuchi, "Topology optimization of compliant mechanisms using the homogenization method," *International Journal for Numerical Methods in Engineering*, vol. 42, pp. 535-559, 1998.
- [88] T. E. Bruns and D. A. Tortorelli, "Topology optimization of non-linear elastic structures and compliant mechanisms," *Computer Methods in Applied Mechanics and Engineering*, vol. 190, pp. 3443-3459, 2001.
- [89] D. Jung and H. C. Gea, "Compliant mechanism design with non-linear materials using topology optimization," *International Journal of Mechanics and Materials in Design*, vol. 1, pp. 157-171, 2004.
- [90] N. M. Patel, A. Tovar, and J. E. Renaud, *Compliant Mechanism Design using the Hybrid Cellular Automaton Method*. Austin, Texas, 2005.
- [91] A. Saxena, "Topology design of large displacement compliant mechanisms with multiple materials and multiple output ports," *Structural and Multidisciplinary Optimization*, vol. 30, pp. 477-490, Dec 2005.
- [92] S. R. Deepak, M. Dinesh, D. K. Sahu, and G. K. Ananthasuresh, "A Comparative Study of the Formulations and Benchmark Problems for the Topology Optimization of Compliant Mechanisms," *Journal of Mechanisms and Robotics*, vol. 1, pp. 011003-1-011003-8, 2009.
- [93] N. M. Patel, B.-S. Kang, J. E. Renaud, and A. Tovar, "Multilevel crashworthiness design using a compliant mechanism approach," in *47th AIAA/ASME/ASCE/AHS/ASC Structures, Structural Dynamics and Materials Conference, May 1, 2006 - May 4, 2006*, Newport, RI, United States, 2006, pp. 5604-5617.
- [94] P. Bandi, J. Schmiedeler, and A. Tovar, "Design of Crashworthy Structures with Controlled Energy Absorption in the HCA Framework," presented at the ASME 2012 International Design Engineering Technical Conferences (IDETC 2012), Chicago, IL, USA, 2012.

- [95] J. I. Craig, "Work and Energy Methods for Structural Analysis," Georgia Institute of Technology 2005.
- [96] K. Maute, S. Schwarz, and E. Ramm, "Adaptive topology optimization of elastoplastic structures," *Structural Optimization*, vol. 15, pp. 81-91, Apr 1998.
- [97] C. C. Swan and I. Kosaka, "Voigt-Reuss topology optimization for structures with nonlinear material behaviors," *International Journal for Numerical Methods in Engineering*, vol. 40, pp. 3785-3814, Oct 1997.
- [98] G. H. Yoon and Y. Y. Kim, "Topology optimization of material-nonlinear continuum structures by the element connectivity parameterization," *International Journal for Numerical Methods in Engineering*, vol. 69, pp. 2196-2218, Mar 2007.
- [99] S. Schwarz and E. Ramm, "Sensitivity analysis and optimization for non-linear structural response," *Engineering Computations*, vol. 18, pp. 610-641, 2001.
- [100] X. D. Huang and Y. M. Xie, "A further review of ESO type methods for topology optimization," *Structural and Multidisciplinary Optimization*, vol. 41, pp. 671-683, May 2010.
- [101] T. E. Bruns, O. Sigmund, and D. A. Tortorelli, "Numerical methods for the topology optimization of structures that exhibit snap-through," *International Journal for Numerical Methods in Engineering*, vol. 55, pp. 1215-1237, Dec 2002.
- [102] C. M. Chia, J. A. Rongong, and K. Worden, "Structural optimisation using a hybrid cellular automata (HCA) algorithm," in *Modern Practice in Stress and Vibration Analysis VI, Proceedings*. vol. 5-6, P. S. Keogh, Ed., ed Stafa-Zurich: Trans Tech Publications Ltd, 2006, pp. 93-100.
- [103] C. Mozumder, J. E. Renaud, and A. Tovar, "Topometry optimisation for crashworthiness design using hybrid cellular automata," *International journal of vehicle design*, vol. 60, pp. 100-120, 2012.
- [104] K. K. Pydimarry, C. K. Mozumder, N. M. Patel, and J. E. Renaud, "Synthesis of a dynamically loaded structure with topology optimization," *SAE International Journal of Passenger Cars - Mechanical Systems*, vol. 2, pp. 1143-1150, 2009.
- [105] A. Tovar, N. M. Patel, A. K. Kaushik, and J. E. Renaud, "Optimality conditions of the hybrid cellular automata for structural optimization," *AIAA journal*, vol. 45, pp. 673-683, 2007.

- [106] A. Tovar, N. M. Patel, G. L. Niebur, M. Sen, and J. E. Renaud, "Topology optimization using a hybrid cellular automaton method with local control rules," *Journal of Mechanical Design*, vol. 128, pp. 1205-1216, 2006.
- [107] K. Khandelwal and A. Tovar, "Control-based topology optimization for structural systems," presented at the Engineering Mechanics Institute (EMI 2010), Los Angeles, California, 2010.
- [108] A. Tovar, "Optimización topológica con la técnica de los autómatas celulares híbridos," *Revista internacional de métodos numéricos para cálculo y diseño en ingeniería*, vol. 21, pp. 365-383, 2005.
- [109] N. Peixinho, N. Jones, and A. Pinho, "Experimental and numerical study in axial crushing of thin walled sections made of high-strength steels," *Journal de Physique IV*, vol. 110, pp. 717-722, 2003.
- [110] V. Tarigopula, M. Langseth, O. S. Hopperstad, and A. H. Clausen, "Axial crushing of thin-walled high-strength steel sections," *International Journal of Impact Engineering*, vol. 32, pp. 847-882, 2006.
- [111] J. Hallquist, *LS-DYNA Theoretical Manual*: Livermore Software Technology Corporation (LSTC), 2006.